



## Global Dynamics of Fractional-order Model for Malaria Disease Transmission

Mlyashimbi Helikumi <sup>a\*</sup> and Paride O. Lolika <sup>b</sup>

<sup>a</sup>Department of Mathematics and Statistics, College of Science and Technical Education, Mbeya University of Science and Technology, P.O.Box 131, Mbeya, Tanzania.

<sup>b</sup> Department of Mathematics, University of Juba, P.O.Box 82, Juba, Central Equatoria, South Sudan.

### Authors' contributions

This work was carried out in collaboration between both authors. Both authors read and approved the final manuscript.

### Article Information

DOI: 10.9734/ARJOM/2022/v18i930409

### Open Peer Review History:

This journal follows the Advanced Open Peer Review policy. Identity of the Reviewers, Editor(s) and additional Reviewers, peer review comments, different versions of the manuscript, comments of the editors, etc are available here: <https://www.sdiarticle5.com/review-history/88271>

Received: 20 April 2022

Accepted: 27 June 2022

Published: 09 July 2022

Original Research Article

## Abstract

In this study, we formulated and analyzed a fractional-order model for malaria disease transmission using Atangana-Beleanu-Caputo in sense to study the effects of heterogeneity vector biting exposure on the human population. To capture effects the heterogeneity vector biting exposure, we sub-divided the human population into two sub-groups namely; the population in high and low risk areas. In the model analysis, we computed the basic reproduction number  $R_0$  and qualitatively used to assess the existence and extinction of disease in the population. Additionally, we used the fixed point theorem to prove the existence and uniqueness of solutions. Numerical schemes for both Euler and Adam-Bathforth-Moulton are present in details and used in model simulations. Furthermore, we performed the numerical simulation to support the analytical results in this study. From numerical simulations, we estimated the values of model parameters using least square fitting method for the real data of malaria reported in Zimbabwe. The sensitivity analysis of the model parameters was done to determine the correlation between model parameters and  $R_0$ . Finally, we used the Euler and Adam-Bashforth-Moulton scheme to simulate the model system using estimated parameters. Overall, we noted that fractional-order derivatives have more influence on the dynamics of malaria disease in the population.

\*Corresponding author: E-mail: [mhelikumi@yahoo.co.uk](mailto:mhelikumi@yahoo.co.uk);

*Keywords:* Malaria; heterogeinity; fractional-order model; model validation.

**2010 Mathematics Subject Classification:** 53C25; 83C05; 57N16.

## 1 Introduction

Malaria is a protozoan disease caused by parasites of the genus *Plasmodium* like *P. falciparum*, *P. malariae*, *P. ovale*, and *P. vivax* [1]. Humans acquire the disease through bites of infected female *Anopheles* mosquitoes and the life cycle of the parasites depends on sexual and asexual phases in mosquitoes and humans respectively [2]. The latest reports released in December 2019 show that close to 230 million malaria cases occurred globally in 2018 alone [2]. Malaria deaths were approximated at 400000 in the same year. Out of the several *Plasmodium* parasites, *P. falciparum* is the most common cause of malaria in Africa and Asia where it is responsible for 80 and 90% of all cases and deaths respectively [3]. The disease is predominant in African countries where it constitutes a huge socioeconomic threat with an estimated annual economic burden of USD 8 billion [4, 5].

Over the years, much scientific research has been undertaken to understand the parasite-vector-host interactions and biology [50]. Nevertheless, the complexities in the parasite's life cycle, coupled with the highly complex social and environmental interactions, and movement of people between endemic and non-endemic areas continue to promote morbidity and mortality from malaria. Although combined global efforts are underway to develop a malaria vaccine [7], [8], [9], [10], there is currently no perfect vaccine against the disease. As such, concerted attempts are still being made to understand malaria disease dynamics and effective control measures.

Mathematical models have been used for more than a century to provide a clear framework for the transmission dynamics of malaria in human populations. The spread of malaria disease in human and mosquito populations has been described mathematically using compartmental models governed by ordinary differential equations (for example, [11], [12], [13]). A number of studies have used the optimal control theory in malaria models. Blayneh *et al.*, [54] developed an optimal control model to study the effects of time-dependent malaria treatment and prevention efforts. Okosun & Makinde [3] also studied a co-infection model of malaria with optimal control. Agosto *et al.*, [15] applied the optimal control theory to study optimal strategies for controlling malaria transmission using treatment, insecticide-treated bed nets and insecticide sprays as control variables, while Gosha *et al.*, [16] proposed a mathematical model to explore the biological control of malaria. In [17] used the optimal control theory to investigate the effects of treatment, larvacide and vaccine in the dynamics of malaria disease transmission. Their results demonstrate that effective and optimal use of preventive measures in the population without use of larvacide the disease can not be eliminated in the population. Authors in [18] assessed the effects of vector reduction, person protection and blood screening strategies in the control of malaria disease in the population. Their results showed the aforementioned controls have the potential to minimize the spread of disease in the population. Additionally, their results also demonstrated that model with standard incidence exhibits back bifurcation and this has an implication in disease eradication in the population. In [19] formulated and analyzed a malaria model with control strategies that interplay between human and mosquito populations. The authors assessed the effects of insecticide-treated bed nets, anti-malaria drugs and social boosting measures in minimizing the spread of the disease in population. Their results revealed that combination of insecticide-treated bed nets and vector control is the most efficient innervation, while the combination of anti-malaria drugs and social boosting measure is the more cost-effective in elimination of the disease in the population. Optimal bed-net and vaccination control efforts in populations with varying levels of naturally acquired immunity were studied by Prosper *et al.*, [20]. Recently, Otieno *et al.*, [21] investigated the malaria transmission dynamics

in Kenya by including time-dependent control measures such as indoor residual spray, treatment, intermittent preventive treatment of malaria in pregnancy, and insecticide treated bed nets. It is clear that several efforts have been made to model malaria transmission dynamics and control. However, the disease still persists in many countries where it is endemic and great source of public health concern. Cognizant of this, it is necessary to continue developing mathematical models of Malaria disease.

Fractional calculus have been classified as generalization of classical calculus and has been utilized as a tool for modeling and investigating the dynamics of real world problems [22]. The most common definitions of fractional calculus are Caputo-fractional and Riemann Liouville operators which are defined by power decay and derivatives as a kernels [23], [24],[58]. These operators have led the existence of Atangana-Baleanu and Caputo-Fabrizio which are not operating under the power-distribution and have non-singular Kernels [52], [15]. The Atangana-Baleanu in Caputo sense is superior and the best option for modeling real world problems including infectious disease compared to Caputo-fabrizio. Additionally, Caputo-Fabrizio which is hinge on power law is not able to capture complex systems while Atangana-Baleanu in Caputo sense, has the properties that kernel is non-singular and non-local which can describe well the behavior of an epidemic models [27]. Fractional calculus have been extensively used for modeling real world problems such as heat conduction, control theory, chaotic theory and biological processes [28],[15]. Fractional order calculus are popular field that describe the application of non-integer order derivative in disease dynamics [29]. From literature, it is believed that modeling of physical and real problems using non-integer order derivative is more precise compared to integer-order derivatives [30],[58]. The main advantages of using fractional order derivative in disease dynamics is that, they can properly capture the memory effects and hereditary properties of species that exist in biological systems [31],[32],[54],[15],[58]. Additional, it is believed that cell membrane of living organisms containing some fractional-order electrical conductance which are classified in the groups of non-integer order models. However, many researchers such engineers, mathematicians, epidemiologist and other scientists are still behind with this knowledge of application of fractional order derivatives in modeling real world problems. Therefore, application of fractional order derivatives is still poorly understood in most of researchers [33], [34], [35],[58]. This paper add knowledge and encourage scientists on using application of Atangana-Baleanu-Caputo operator in modeling real world problems.

Mathematical models of infectious disease using fractional order via Atangana-Baleanu derivative have been formulated and analyzed in order to explore the dynamics of disease in the population and references cited therein (see, [28], [36], [37], [38]). Khan *et al.*, [28] formulated and studied a new fractional order model for tuberculosis with relapse via Atangana-Baleanu derivative. From the model analysis they proved the existence and uniqueness of model solution using point fixed theorem. In [36], formulated and studied a fractional order model for Hepatitis B virus using Atangana-baleanu in cuputo sense.

Motivated by the previous study on fractional order models via Atangana-Baleanu derivative, the present study was designed to develop a fractional order model using Atangana-Baleanu Cuputo (ABC) in sense to study malaria transmission dynamics with heterogeneity. The main advantage of using ABC operator fractional order derivative with respect to another function is that, it has a non-local and non-singular kernel [39],[40],[33],[41]. This provide suitable classification differentiation operator and suitable function in modeling real world-problems such as infectious diseases [52]. The organization of the paper is as follows: section 2 discusses the model formulation and analytical results. The numerical simulation of the model is presented in section 3, while the concluding remarks are in Section 4.

## 2 Model Formulation and Analytical Results

### 2.1 Mathematical model

In this paper, we formulated and studied a new fractional-order model which is an extension of the classical model studied in [42]. The model take into account the interplay between vector (mosquitoes) and human populations governed by the following assumptions:

- (i) The vector population is sub-divided into three compartments: susceptible  $S_v(t)$ , exposed  $E_v(t)$  and infected  $I_v(t)$ . Thus, the total population of vector is denoted by  $N_v(t)$  and defined by:  $N_v(t) = S_v(t) + E_v(t) + I_v(t)$ . We denote the subscript  $v$  and  $h$  throughout the document to represent the parameters and variables for vectors and humans respectively.
- (ii) The total human population is denoted by  $N_h(t)$  and is sub-divided into two sub-groups according the exposure to heterogeneous vector biting, we denote  $N_{h1}(t)$  and  $N_{h2}(t)$  to represent the total human population in high and low risk areas respectively, thus,  $N_h(t) = N_{h1}(t) + N_{h2}(t)$ . The human population in both low and high risk areas is sub-divided into five non-intersecting compartments: susceptible  $S_{hi}(t)$ , exposed  $E_{hi}(t)$ , infected with symptomatic disease (severe and clinical cases)  $I_{hi}(t)$ , infected with asymptomatic disease  $A_{hi}(t)$  and temporary immune individuals  $R_{hi}(t)$  for  $i = 1, 2$ . With these divisions, the total human populations in both low and high risk areas at time  $t$  are given as,  $N_{h1}(t) = S_{h1}(t) + E_{h1}(t) + I_{h1}(t) + A_{h1}(t) + R_{h1}(t)$ ,  $N_{h2}(t) = S_{h2}(t) + E_{h2}(t) + I_{h2}(t) + A_{h2}(t) + R_{h2}(t)$ .
- (iii) The average life span of humans in malaria endemic regions is  $1/\mu_{hi}^\alpha$ , where  $\mu_{hi}^\alpha$  is the natural mortality rate of humans for  $i = 1; 2$ . Similarly, the average life span of mosquitoes is  $1/\mu_v^\alpha$ , where  $\mu_v^\alpha$  is the natural mortality rate of mosquitoes. The recruitment rates of susceptible human and mosquito populations are denoted by  $\Lambda_{hi}^\alpha$  for  $i = 1; 2$ ,  $\Lambda_v^\alpha$ , respectively. Human recruitment consists of new births and immigration. The susceptible human population increases due to natural recovery and treatment of symptomatically infected individuals at the rate  $\theta_{hi}^\alpha \gamma_{hi}^\alpha$  for  $i = 1; 2$ . Temporary immune individuals move to the susceptible class after losing their immunity at the rate  $\gamma_{ui}^\alpha$ , hence  $\frac{1}{\gamma_{ui}^\alpha}$  for  $i = 1; 2$  is the average duration of immunity.
- (iv) The exposed human and vector populations grow as a result of new infections and decline due to natural mortality and move to the infected classes at the rate  $\gamma_{ei}^\alpha$  for  $i = 1; 2$ . For humans and  $\gamma_v^\alpha$  for vectors. It is assumed that a proportion of the exposed human class ( $\rho_i^\alpha \gamma_{ei}^\alpha$  ( $0 \leq \rho_i^\alpha \leq 1$ )) is developing a symptomatic disease, while the rest ( $(1 - \rho_i^\alpha) \gamma_{ei}^\alpha$ ) is still asymptomatic. The infected human population with symptomatic disease (severe and clinical cases)  $I_{hi}(t)$  decreases as a result of natural death and is further reduced by disease-related mortality at a rate  $\delta_{hi}^\alpha$ . By clinical treatment or natural recovery, a proportion of the infected population  $\theta_{hi}^\alpha \gamma_{hi}^\alpha$  returns to the susceptible state while the rest moves to the asymptomatic state at the rate  $(1 - \rho_{hi}^\alpha) \gamma_{hi}^\alpha$ . Those in the asymptomatic state may additionally develop disease through superinfection at rate  $\rho_i \lambda_{hi}^\alpha(t)$ .
- (v) In this framework, we assume that the transmission of infection in humans occurs solely when susceptible individuals are bitten by an infectious vector and the disease transmission rate is modeled by the equation (2.1):

$$\lambda_{hi}^\alpha(t) = \frac{\beta_h^\alpha I_v(t)}{N_{hi}(t)}, \lambda_v^\alpha = \frac{\beta_v^\alpha (I_{hi}(t) + \sigma_i A_{hi}(t))}{N_{hi}(t)}$$

The parameter  $\beta_h^\alpha$  is the effective contact rate of humans, and is defined as the product of the average number of mosquito bites received by humans and the probability of transmission from an infectious human to a susceptible mosquito. Similarly,  $\beta_v^\alpha$  is the effective contact rate of vectors which is defined as the product of the biting rate of mosquitoes and the probability of transmission

per bite from an infectious mosquito to a susceptible human. Susceptible individuals who are rich assumed to have reduced chances of infection modelled by  $(1 - \epsilon_h^\alpha)$  with  $0 < \epsilon_h^\alpha < 1$ . A reduction in susceptibility is attributed to the fact that because some can afford mosquito nets and repellents because they are rich. We denote the rate of individual progression to high and low risk area by  $p_{h1}^\alpha$  and  $p_{h2}^\alpha$  respectively

**Definition 1.** (see [43]), given the function  $y \in \mathcal{H}'(0, T), T > 0$  and  $\alpha \in (0, 1]$ , the fractional operator:

${}^{ABC}D_{0+}^\alpha y(t) = \frac{M(\alpha)}{1-\alpha} \int_0^t E_\alpha\left(\frac{-\alpha}{1-\alpha}(t-\tau)^\alpha\right) y'(\tau) d\tau$  is called ABC-fractional operator where  $M(\alpha)$  denotes the normalization and satisfies  $M(0) = M(1) = 1$  and  $E_\alpha(\cdot)$  denotes the Mittag-Leffler function of the form:  $E_\alpha(v) = \sum_{k=0}^\infty \frac{v^k}{\Gamma(\alpha k + 1)}$

**Definition 2.** (see [43]) the fractional operator;

$${}^{ABC}I_{0+}^\alpha z(t) = \frac{1-\alpha}{M(\alpha)} z(t) + \frac{\alpha}{M(\alpha)\Gamma(\alpha)} \int_0^t (t-\tau)^{1-\alpha} z(\tau) d\tau, t > 0$$

is called the integral operator of sense ABC-fractional derivatives.

Based on the above assumptions and definitions, the proposed model in the sense of ABC-fractional derivatives, for  $i, j = 1, 2$  is given as follows:

$$\left. \begin{aligned} {}^{ABC}D_0^\alpha S_{hi}(t) &= \Lambda_{hi}^\alpha - \frac{\beta_h^\alpha S_{hi}(t) I_v(t)}{N_{hi}(t)} - \mu_{hi}^\alpha S_{hi}(t) - p_{h1}^\alpha S_{hi}(t) + p_{hj}^\alpha S_{hj}(t) \\ &\quad + \gamma_{ui}^\alpha R_{hi}(t) + \theta_{hi}^\alpha \gamma_{hi}^\alpha I_{hi}(t), \\ {}^{ABC}D_0^\alpha E_{hi}(t) &= \frac{\beta_h^\alpha S_{hi}(t) I_v(t)}{N_{hi}(t)} - \mu_{hi}^\alpha E_{hi}(t) - \gamma_{ei}^\alpha E_{hi}(t), \\ {}^{ABC}D_0^\alpha I_{hi}(t) &= \rho_i^\alpha \gamma_{ei}^\alpha E_{hi}(t) + \frac{\rho_i^\alpha \beta_h^\alpha A_{hi}(t) I_v(t)}{N_{hi}(t)} - (\mu_{hi}^\alpha + \delta_{hi}^\alpha + \gamma_{hi}^\alpha) I_{hi}(t), \\ {}^{ABC}D_0^\alpha A_{hi}(t) &= (1 - \rho_h^\alpha) \gamma_{ei}^\alpha E_{hi}(t) - \frac{\rho_i^\alpha \beta_h^\alpha A_{hi}(t) I_v(t)}{N_{hi}(t)} + (1 - \theta_h^\alpha) \gamma_{hi}^\alpha I_{hi}(t) - \gamma_{ai}^\alpha A_{hi}(t) \\ &\quad - \mu_{hi}^\alpha A_{hi}(t), \\ {}^{ABC}D_0^\alpha R_{hi}(t) &= \gamma_{ai}^\alpha A_{hi}(t) - (\mu_{hi}^\alpha + \gamma_{ui}^\alpha) R_{hi}(t). \end{aligned} \right\}$$

$$\left. \begin{aligned} {}^{ABC}D_0^\alpha S_v(t) &= \Lambda_v^\alpha - \frac{\beta_v^\alpha S_v(t) (I_{hi}(t) + \sigma_i^\alpha A_{hi})}{N_{h1}} - \frac{(1 - \epsilon_h^\alpha) \beta_v^\alpha S_v(t) (I_{hj}(t) + \sigma_j^\alpha A_{hj})}{N_{hj}} \\ &\quad - \mu_v^\alpha S_v(t), \\ {}^{ABC}D_0^\alpha E_v(t) &= \frac{\beta_v^\alpha S_v(t) (I_{hi}(t) + \sigma_i^\alpha A_{hi})}{N_{hi}} + \frac{\beta_v^\alpha S_v(t) (I_{hj}(t) + \sigma_j^\alpha A_{hj})}{N_{hj}} - (\mu_v^\alpha + \gamma_v^\alpha) E_v(t), \\ {}^{ABC}D_0^\alpha I_v(t) &= \gamma_v^\alpha E_v(t) - \mu_v^\alpha I_v(t). \end{aligned} \right\} \tag{2.1}$$

and  $S_{hi}(0) = S_{h(i,0)}, E_{hi}(0) = E_{h(i,0)}, I_{hi}(0) = I_{h(i,0)}, A_{hi}(0) = A_{h(i,0)}, R_{hi}(0) = R_{h(i,0)}, S_v(0) = S_{v0}, E_v(0) = E_{v0}, I_v(0) = I_{v0}$ . Where  $0 < \alpha \leq 1$  and  ${}^{ABC}D_0^\alpha$  is Atangana-Beleanu in Caputo sense of order  $\alpha$ .

## 2.2 Model analysis

### 2.2.1 Non-negativity and boundness of model solutions

**Theorem 1.** For the model system (2.1), there exists a unique solution in  $(0, \infty)$ , however, the solution is always positive for all values of  $t \geq 0$  and remains in  $\mathcal{R}_+^2$ .

*Proof.* From the model system (2.1), for  $i, j = 1, 2$  we first show that:

$\mathcal{R}_+^2 = \{(N_{hi}, N_v) \in \mathcal{R}_+^2 : N_{hi} \geq 0, N_v \geq 0\}$  is a positive invariant. Now we have to demonstrate that each hyper-plane bounding the positive orthant and the vector field points to  $\mathcal{R}_+^3$ . Let us consider the following cases:

Case 1: Let us assume that there exists a  $t_* > t_0$  such that  $N_{hi}(t_*) = 0$ , and  $N_{hi}(t) < 0$  for  $t \in (t_*, t_1)$ , where  $t_1$  is sufficiently close to  $t_*$ , if  $N_{hi}(t_*) = 0$ , then we have that:

${}^{ABC}D_0^\alpha N_{hi}(t_*) = \Lambda_{hi}^\alpha - \mu_{hi}^\alpha N_{hi} + p_{hj}^\alpha S_{hj} + p_{hi}^\alpha S_{hi} > 0$ . This implies that  ${}^cD_t^\alpha N_{hi}(t) > 0$  for all  $t \in [t_*, t_1]$ .

Case 2: Let us assume that there exists a  $t_* > t_0$  such that  $N_v(t_*) = 0$ , and  $N_v(t) < 0$  for  $t \in (t_*, t_1)$ , where  $t_1$  is sufficiently close to  $t_*$ , if  $N_v(t_*) = 0$ , then we have that:

${}^{ABC}D_0^\alpha N_v(t_*) = \Lambda_v^\alpha - \mu_v^\alpha N_v > 0$ . This implies that  ${}^{ABC}D_0^\alpha N_v(t) > 0$  for all  $t \in [t_*, t_1]$ .

The above discussion show that the three hyper-plane bounding the orthants, that is the vector field points to  $\mathbb{R}_+^3$ . This show that all the solutions of the model system (2.1) remain positive for all  $t \geq 0$ .  $\square$

**Theorem 2.** Let  $\Phi(t) = (N_{hi}(t), N_v(t))$  be the unique solution of the model system (2.1) for all  $t \geq 0$ , then the solution  $\Phi(t)$  is bounded above, that is,  $\Phi(t) \in \Omega$  where  $\Omega$  is the feasible region defined as:

$$\Omega = \left\{ \begin{pmatrix} N_{hi}(t) \\ N_v(t) \end{pmatrix} \in \mathbb{R}_+^2 \mid \begin{array}{l} 0 \leq N_{hi}(t) \leq C_{hi}, \\ 0 \leq N_v(t) \leq C_v \end{array} \right\}$$

which is interior denoted by  $int(\Omega)$  and given by:

$$int(\Omega) = \left\{ \begin{pmatrix} N_{hi}(t) \\ N_v(t) \end{pmatrix} \in \mathbb{R}_+^2 \mid \begin{array}{l} 0 < N_{hi}(t) < C_{hi}, \\ 0 < N_v(t) < C_v \end{array} \right\}$$

*Proof.* Here we prove that the solutions of model system (2.1) are bounded for all  $t \geq 0$ . Biologically, the least possible value of each state of the model system (2.1) is zero. Next, we determine the upper-bound of the states. Based on this discussion, it easy to show that the following conditions hold for biological relevance of species.  $0 \leq N_{hi}(t) \leq C_{hi}$ , and  $0 \leq N_v(t) \leq C_v$ . From these conditions, we have:

$${}^{ABC}D_0^\alpha N_{hi} \leq \Lambda_{hi}^\alpha - \mu_{hi}^\alpha N_{hi}(t)$$

Using the Laplace transformation conditions, we have:

$$S^\alpha L[N_{hi}(t)] - S^{\alpha-1} N_{hi}(0) \leq \frac{\Lambda_{hi}^\alpha}{S} - \mu_{hi}^\alpha L[N_{hi}(t)]$$

Collecting the likely terms, we have:

$$\begin{aligned} L[N_{hi}(t)] &\leq \Lambda_{hi}^\alpha \frac{S^{-1}}{S^\alpha + \mu_{hi}^\alpha} + N_{hi}(0) \frac{S^{\alpha-1}}{S^\alpha + \mu_{hi}^\alpha} \\ &= \Lambda_{hi}^\alpha \frac{S^{\alpha-(1+\alpha)}}{S^\alpha + \mu_{hi}^\alpha} + N_{hi}(0) \frac{S^{\alpha-1}}{S^\alpha + \mu_{hi}^\alpha} \end{aligned}$$

Using the inverse Laplace transform, we have:

$$\begin{aligned} N_{hi}(t) &\leq L^{-1} \left\{ \Lambda_{hi}^\alpha \frac{S^{\alpha-(1+\alpha)}}{S^\alpha + \mu_{hi}^\alpha} \right\} - N_{hi}(0) L^{-1} \left\{ \frac{S^{\alpha-1}}{S^\alpha + \mu_{hi}^\alpha} \right\} \\ &\leq \Lambda_{hi}^\alpha t^\alpha E_{\alpha, \theta+1}(-\mu_{hi}^\alpha) t^\alpha + N_{hi}(0) E_{\alpha, 1}(-\mu_{hi}^\alpha) t^\alpha \\ &\leq \frac{\Lambda_{hi}^\alpha}{\mu_{hi}^\alpha} t^\alpha E_{\alpha, \alpha+1}(-\mu_{hi}^\alpha) t^\alpha + N_{hi}(0) E_{\alpha, 1}(-\mu_{hi}^\alpha) t^\alpha \\ &\leq Max \left\{ \frac{\Lambda_{hi}^\alpha}{\mu_{hi}^\alpha}, N_{hi}(0) \right\} \left( t^\alpha E_{\alpha, \alpha+1}(-\mu_{hi}^\alpha) t^\alpha + E_{\alpha, 1}(-\mu_{hi}^\alpha) t^\alpha \right) \end{aligned}$$

$$= \frac{C}{\Gamma(1)} = C_{hi}.$$

Where  $C_{hi} = \text{Max}\left\{\frac{\Lambda_{hi}^\alpha}{\mu_{hi}^\alpha}, N_{hi}(0)\right\}$ . Therefore,  $N_{hi}(t)$  is bounded above. From the vector population, we have:

$${}^{ABC}D_0^\alpha N_v \leq \Lambda_v^\alpha - \mu_v^\alpha N_v(t)$$

Using the Laplace transformation conditions, we have:

$$S^\alpha L[N_v(t)] - S^{\alpha-1} N_v(0) \leq \frac{(1 - p_v^\alpha)\Lambda_v^\alpha}{S} - \mu_v^\alpha L[N_v(t)]$$

Collecting the likely terms we have

$$\begin{aligned} L[N_v(t)] &\leq \Lambda_v^\alpha \frac{S^{-1}}{S^\alpha + \mu_v^\alpha} + N_v(0) \frac{S^{\alpha-1}}{S^\alpha + \mu_v^\alpha} \\ &= \Lambda_v^\alpha \frac{S^{\alpha-(1+\alpha)}}{S^\alpha + \mu_v^\alpha} + N_v(0) \frac{S^{\alpha-1}}{S^\alpha + \mu_v^\alpha} \end{aligned}$$

Using the inverse Laplace transform, we have:

$$\begin{aligned} N_v(t) &\leq L^{-1}\left\{\Lambda_v^\alpha \frac{S^{\alpha-(1+\alpha)}}{S^\alpha + \mu_v^\alpha}\right\} - N_v(0)L^{-1}\left\{\frac{S^{\alpha-1}}{S^\alpha + \mu_v^\alpha}\right\} \\ &\leq \Lambda_v^\alpha t^\alpha E_{\alpha,\alpha+1}(-\mu_v^\alpha)t^\alpha + N_v(0)E_{\alpha,1}(-\mu_v^\alpha)t^\alpha \\ &\leq \frac{\Lambda_v^\alpha}{\mu_v^\alpha} t^\alpha E_{\alpha,\alpha+1}(-\mu_v^\alpha)t^\alpha + N_v(0)E_{\alpha,1}(-\mu_v^\alpha)t^\alpha \\ &\leq \text{Max}\left\{\frac{\Lambda_v^\alpha}{\mu_v^\alpha}, N_v(0)\right\} \left(t^\alpha E_{\alpha,\alpha+1}(-\mu_v^\alpha)t^\alpha + E_{\alpha,1}(-\mu_v^\alpha)t^\alpha\right) \\ &= \frac{C}{\Gamma(1)} = C_v. \end{aligned}$$

Where  $C_v = \text{Max}\left\{\frac{\Lambda_v^\alpha}{\mu_v^\alpha}, N_v(0)\right\}$ . Therefore,  $N_v(t)$  is bounded above and this complete the proof.  $\square$

### 2.3 The basic reproduction number and existence of equilibria

In this section, we compute the threshold quantity  $\mathcal{R}_0$  which determines the power of disease to spread in the population. The model system (2.1) always has a disease-free equilibrium  $\mathcal{E}^0$  given by:

$$\mathcal{E}^0 : \left( S_{h1}^0, E_{h1}^0, I_{h1}^0, A_{h1}^0, S_{h2}^0, E_{h2}^0, I_{h2}^0, A_{h2}^0, S_v^0, E_v^0, I_v^0 \right) = \left( S_{h1}^0, 0, 0, 0, S_{h2}^0, 0, 0, 0, S_v^0, 0, 0 \right).$$

Where by:

$$\left. \begin{aligned} S_{h1}^0 &= \frac{\Lambda_{h1}^\alpha}{\mu_{h1}^\alpha + p_{h1}^\alpha} + \frac{p_{h2}^\alpha \Lambda_{h2}^\alpha (\mu_{h1}^\alpha + p_{h1}^\alpha) + p_{h1}^\alpha p_{h2}^\alpha \Lambda_{h1}^\alpha}{(\mu_{h1}^\alpha + p_{h1}^\alpha)((\mu_{h1}^\alpha + p_{h1}^\alpha)(\mu_{h2}^\alpha + p_{h2}^\alpha) - p_{h1}^\alpha p_{h2}^\alpha)}, \\ S_{h2}^0 &= \frac{\Lambda_{h2}^\alpha (\mu_{h1}^\alpha + p_{h1}^\alpha + p_{h1}^\alpha \Lambda_{h1}^\alpha)}{\mu_{h2}^\alpha (\mu_{h1}^\alpha + p_{h1}^\alpha) + p_{h2}^\alpha (\mu_{h2}^\alpha + p_{h2}^\alpha) - p_{h1}^\alpha p_{h2}^\alpha}, \\ S_v^0 &= \frac{\Lambda_v^\alpha}{\mu_v^\alpha}. \end{aligned} \right\} \quad (2.2)$$

Following the next generation matrix approach as used in [?], [51], the non-negative matrix  $\mathcal{F}$  that denotes the generation of new infection and the non-singular matrix  $\mathcal{V}$  that denotes the disease transfer among compartments evaluated at  $\mathcal{E}^0$  are defined as follows:

$$\mathcal{F} = \begin{pmatrix} 0 & 0 & 0 & 0 & 0 & 0 & 0 & \beta_h^\alpha \\ 0 & 0 & 0 & 0 & 0 & 0 & 0 & 0 \\ 0 & 0 & 0 & 0 & 0 & 0 & 0 & 0 \\ 0 & 0 & 0 & 0 & 0 & 0 & 0 & (1 - \epsilon_h^\alpha)\beta_h^\alpha \\ 0 & 0 & 0 & 0 & 0 & 0 & 0 & 0 \\ 0 & \frac{\beta_v S_v^0}{S_{h1}^0} & \frac{\beta_v S_v^0}{S_{h1}^0} \sigma_1^\alpha & 0 & \frac{(1 - \epsilon_h^\alpha)\beta_v S_v^0}{S_{h2}^0} & \frac{(1 - \epsilon_h^\alpha)\beta_v S_v^0}{S_{h2}^0} \sigma_2^\alpha & 0 & 0 \\ 0 & 0 & 0 & 0 & 0 & 0 & 0 & 0 \end{pmatrix} \quad (2.3)$$

$$\mathcal{V} = \begin{pmatrix} \mu_h^\alpha + \gamma_{e1}^\alpha & 0 & 0 & 0 & 0 & 0 & 0 & 0 & 0 \\ -\alpha_h^\alpha \gamma_{e1}^\alpha & \mu_{h1}^\alpha + \delta_{h1}^\alpha + \gamma_{h1}^\alpha & 0 & 0 & 0 & 0 & 0 & 0 & 0 \\ -(1 - \alpha_h^\alpha)\gamma_{e1}^\alpha & -(1 - \theta_{h1}^\alpha)\gamma_{h1}^\alpha & \mu_{h1}^\alpha + \gamma_{a1}^\alpha & 0 & 0 & 0 & 0 & 0 & 0 \\ 0 & 0 & 0 & 0 & \mu_{h2}^\alpha + \gamma_{e2}^\alpha & 0 & 0 & 0 & 0 \\ 0 & 0 & 0 & 0 & -\alpha_h^\alpha \gamma_{e2}^\alpha & n_1 & 0 & 0 & 0 \\ 0 & 0 & 0 & 0 & -(1 - \alpha_h^\alpha)\gamma_{e2}^\alpha & n_2 & n_3 & 0 & 0 \\ 0 & 0 & 0 & 0 & 0 & 0 & 0 & n_4 & 0 \\ 0 & 0 & 0 & 0 & 0 & 0 & 0 & -\gamma_v^\alpha & \mu_v^\alpha \end{pmatrix} \quad (2.4)$$

with  $n_1 = \mu_{h2}^\alpha + \delta_{h2}^\alpha + \gamma_{h2}^\alpha$ ,  $n_2 = -(1 - \theta_{h2}^\alpha)\gamma_{h2}^\alpha$ ,  $n_3 = \gamma_{a2}^\alpha + \mu_{h2}^\alpha$ ,  $n_4 = \mu_v^\alpha + \gamma_v^\alpha$ . Therefore, from (2.3) and (2.4) it can easily be verified that the basic reproduction number of system (2.1) is given as:

$$\mathcal{R}_0 = \sqrt{M_1 M_2 + M_3 M_4},$$

with:

$$\begin{aligned} M_1 &= \frac{\beta_h^\alpha \gamma_v^\alpha}{(\mu_v^\alpha + \gamma_v^\alpha)\mu_v^\alpha}, \\ M_2 &= \frac{\beta_h^\alpha S_v^0 \alpha_1^\alpha \gamma_{e1}^\alpha}{S_{h1}^0 (\mu_{h1}^\alpha + \gamma_{e1}^\alpha)(\mu_{h1}^\alpha + \delta_{h1}^\alpha + \gamma_{h1}^\alpha)} + \frac{\beta_v^\alpha S_v^0 \sigma_1^\alpha}{S_{h1}^0} \mathcal{A}_1, \\ M_3 &= \frac{(1 - \epsilon_h^\alpha)\beta_h^\alpha \gamma_v^\alpha}{(\mu_v^\alpha + \gamma_v^\alpha)\mu_v^\alpha}, \\ M_4 &= \frac{(1 - \epsilon_h^\alpha)\beta_h^\alpha S_v^0 \alpha_h^\alpha \gamma_{e2}^\alpha}{S_{h2}^0 (\mu_{h2}^\alpha + \gamma_{e2}^\alpha)(\mu_{h2}^\alpha + \delta_{h2}^\alpha + \gamma_{h2}^\alpha)} + \frac{(1 - \epsilon_h^\alpha)\beta_v^\alpha S_v^0 \sigma_2^\alpha}{S_{h2}^0} \mathcal{A}_2, \\ \mathcal{A}_1 &= \frac{(\mu_{h1}^\alpha + \delta_{h1}^\alpha + \gamma_{h1}^\alpha)(1 - \alpha_h^\alpha)\gamma_{e1}^\alpha + \alpha_h^\alpha \gamma_{e1}^\alpha (1 - \theta_{h1}^\alpha)\gamma_{h1}^\alpha}{(\mu_{h1}^\alpha + \delta_{h1}^\alpha + \gamma_{h1}^\alpha)(\mu_{h1}^\alpha + \gamma_{e1}^\alpha)(\mu_{h1}^\alpha + \gamma_{a1}^\alpha)}, \text{ and} \\ \mathcal{A}_2 &= \frac{(\mu_{h2}^\alpha + \delta_{h2}^\alpha + \gamma_{h2}^\alpha)(1 - \alpha_h^\alpha)\gamma_{e2}^\alpha + \alpha_h^\alpha \gamma_{e2}^\alpha (1 - \theta_{h2}^\alpha)\gamma_{h2}^\alpha}{(\mu_{h2}^\alpha + \delta_{h2}^\alpha + \gamma_{h2}^\alpha)(\mu_{h2}^\alpha + \gamma_{e2}^\alpha)(\mu_{h2}^\alpha + \gamma_{a2}^\alpha)}. \end{aligned}$$



The basic reproduction number  $\mathcal{R}_0$  is defined as the expected number of secondary cases (vector or host) produced in a completely susceptible population, by one infectious individual (vector or host respectively) during its lifetime as infectious. The square root here is due to the fact that the generation of secondary cases in vector-borne diseases require two transmission process.

### 2.4 Existence and uniqueness of solution

In this section, we study the existence and uniqueness of solution of the model system (2.1) using the techniques of fixed point theorem. First, we denote the Banach space of all continuous real-valued function equipped with the norm by  $\mathcal{B} = \ell([0, T], \mathfrak{R})$ , defined as:

$$\|S_{hi}, E_{hi}, I_{hi}, R_{hi}, A_{hi}, S_v, E_v, I_v\| = \|S_{hi}\| + \|E_{hi}\| + \|I_{hi}\| + \|R_{hi}\| + \|A_{hi}\| + \|S_v\| + \|E_v\| + \|I_v\|,$$

where:

$$\begin{aligned} \|S_{hi}(t)\| &= \sup_{t \in [0, T]} |S_{hi}(t)|, & \|E_{hi}(t)\| &= \sup_{t \in [0, T]} |E_{hi}(t)|, & \|I_{hi}(t)\| &= \sup_{t \in [0, T]} |I_{hi}(t)|, \\ \|R_{hi}(t)\| &= \sup_{t \in [0, T]} |R_{hi}(t)|, & \|A_{hi}(t)\| &= \sup_{t \in [0, T]} |A_{hi}(t)|, & \|S_v(t)\| &= \sup_{t \in [0, T]} |S_v(t)|, \\ \|E_v(t)\| &= \sup_{t \in [0, T]} |E_v(t)|, & \|I_v(t)\| &= \sup_{t \in [0, T]} |I_v(t)|. \end{aligned}$$

In what follows, we utilize the fractional integral operator  ${}^{AB}I_{0+}^\alpha$  on both sides of the system (2.1), for  $i, j = 1, 2$  we get:

$$\left. \begin{aligned} S_{hi}(t) - S_{hi}(0) &= {}^{AB}I_{0+}^\alpha \left\{ \Lambda_{hi}^\alpha - \frac{\beta_h^\alpha S_{hi}(t) I_v(t)}{N_{hi}(t)} - \mu_{hi}^\alpha S_{hi}(t) - p_{hi}^\alpha S_{hi}(t) + p_{hj}^\alpha S_{hj}(t) \right. \\ &\quad \left. + \gamma_{u1}^\alpha R_{hi}(t) + \theta_{hi}^\alpha \gamma_{hi}^\alpha I_{hi}(t) \right\}, \\ E_{hi}(t) - E_{hi}(0) &= {}^{AB}I_{0+}^\alpha \left\{ \frac{\beta_h^\alpha S_{hi}(t) I_v(t)}{N_{hi}(t)} - \mu_{hi}^\alpha E_{hi}(t) - \gamma_{ei}^\alpha E_{hi}(t) \right\}, \\ I_{hi}(t) - I_{hi}(0) &= {}^{AB}I_{0+}^\alpha \left\{ \rho_h^\alpha \gamma_{ei}^\alpha E_{hi}(t) + \frac{\rho_i^\alpha \beta_h^\alpha A_{hi}(t) I_v(t)}{N_{hi}(t)} - (\mu_{hi}^\alpha + \delta_{hi}^\alpha + \gamma_{hi}^\alpha) I_{hi}(t) \right\}, \\ A_{hi}(t) - A_{hi}(0) &= {}^{AB}I_{0+}^\alpha \left\{ (1 - \rho_h^\alpha) \gamma_{ei}^\alpha E_{hi}(t) - \frac{\rho_i^\alpha \beta_h^\alpha A_{hi}(t) I_v(t)}{N_{hi}(t)} + (1 - \theta_{hi}^\alpha) \gamma_{hi}^\alpha I_{hi}(t) \right. \\ &\quad \left. - \gamma_{ai}^\alpha A_{hi}(t) - \mu_{hi}^\alpha A_{hi}(t) \right\}, \\ R_{hi}(t) - R_{hi}(0) &= {}^{AB}I_{0+}^\alpha \left\{ \gamma_{ai}^\alpha A_{hi}(t) - (\mu_{hi}^\alpha + \gamma_{ui}^\alpha) R_{hi}(t) \right\}, \end{aligned} \right\} \tag{2.5}$$

$$\left. \begin{aligned} S_v(t) - S_v(0) &= {}^{AB}I_{0+}^\alpha \left\{ \Lambda_v^\alpha - \frac{\beta_v^\alpha S_v(t) (I_{hi}(t) + \sigma_i^\alpha A_{hi})}{N_{hi}} - \frac{(1 - \epsilon_h) \beta_v^\alpha S_v(t) (I_{hj}(t) + \sigma_j^\alpha A_{hj})}{N_{hj}} \right. \\ &\quad \left. - \mu_v^\alpha S_v(t) \right\}, \\ E_v(t) - E_v(0) &= {}^{AB}I_{0+}^\alpha \left\{ \frac{\beta_v^\alpha S_v(t) (I_{hi}(t) + \sigma_i^\alpha A_{hi})}{N_{hi}} + \frac{(1 - \epsilon_h) \beta_v^\alpha S_v(t) (I_{hj}(t) + \sigma_j^\alpha A_{hj})}{N_{hj}} \right. \\ &\quad \left. - (\mu_v^\alpha + \gamma_v^\alpha) E_v(t) \right\}, \\ I_v(t) - I_v(0) &= {}^{AB}I_{0+}^\alpha \left\{ \gamma_v^\alpha E_v(t) - \mu_v^\alpha I_v(t) \right\}. \end{aligned} \right\} \tag{2.6}$$

Which implies that, for  $k = 1, 2, 3 \dots 13$  we have:

$$\left. \begin{aligned} S_{hi}(t) &= S_{hi}(0) + \frac{(1-\alpha)}{M(\alpha)}(F_i(t, S_{hi}(t))) + \frac{\alpha}{M(\alpha)} \frac{1}{\Gamma(\alpha)} \int_0^t F_k(t, S_{hi}(t))d\tau, \\ E_{hi}(t) &= E_{hi}(0) + \frac{(1-\alpha)}{M(\alpha)}(F_k(t, E_{hi}(t))) + \frac{\alpha}{M(\alpha)} \frac{1}{\Gamma(\alpha)} \int_0^t F_k(t, E_{hi}(t))d\tau, \\ I_{hi}(t) &= I_{hi}(0) + \frac{(1-\alpha)}{M(\alpha)}(F_k(t, I_{hi}(t))) + \frac{\alpha}{M(\alpha)} \frac{1}{\Gamma(\alpha)} \int_0^t F_k(t, I_{hi}(t))d\tau, \\ R_{hi}(t) &= R_{hi}(0) + \frac{(1-\alpha)}{M(\alpha)}(F_k(t, R_{hi}(t))) + \frac{\alpha}{M(\alpha)} \frac{1}{\Gamma(\alpha)} \int_0^t F_k(t, R_{hi}(t))d\tau, \\ A_{hi}(t) &= A_{hi}(0) + \frac{(1-\alpha)}{M(\alpha)}(F_k(t, A_{hi}(t))) + \frac{\alpha}{M(\alpha)} \frac{1}{\Gamma(\alpha)} \int_0^t F_k(t, A_{hi}(t))d\tau, \\ S_v(t) &= S_v(0) + \frac{(1-\alpha)}{M(\alpha)}(F_k(t, S_v(t))) + \frac{\alpha}{M(\alpha)} \frac{1}{\Gamma(\alpha)} \int_0^t F_k(t, S_v(t))d\tau, \\ E_v(t) &= E_v(0) + \frac{(1-\alpha)}{M(\alpha)}(F_k(t, E_v(t))) + \frac{\alpha}{M(\alpha)} \frac{1}{\Gamma(\alpha)} \int_0^t F_k(t, E_v(t))d\tau, \\ I_v(t) &= I_v(0) + \frac{(1-\alpha)}{M(\alpha)}(F_k(t, I_v(t))) + \frac{\alpha}{M(\alpha)} \frac{1}{\Gamma(\alpha)} \int_0^t F_k(t, I_v(t))d\tau. \end{aligned} \right\} \tag{2.7}$$

Where:

$$\left. \begin{aligned} F_k(t, S_{hi}(t)) &= \Lambda_{hi}^\alpha - \frac{\beta_h^\alpha S_{hi}(t)I_v(t)}{N_{hi}(t)} - \mu_{hi}^\alpha S_{hi}(t) - p_{hi}^\alpha S_{hi}(t) + p_{hj}^\alpha S_{hj}(t) \\ &\quad + \gamma_{ui}^\alpha R_{hi}(t) + \theta_{hi}^\alpha \gamma_{hi}^\alpha I_{hi}(t), \\ F_k(t, E_{hi}(t)) &= \frac{\beta_h^\alpha S_{hi}(t)I_v(t)}{N_{hi}(t)} - \mu_{hi}^\alpha E_{hi}(t) - \gamma_{ei}^\alpha E_{hi}(t), \\ F_k(t, I_{hi}(t)) &= \rho_{ei}^\alpha \gamma_{ei}^\alpha E_{hi}(t) + \frac{\rho_i^\alpha \beta_h^\alpha A_{hi}(t)I_v(t)}{N_{hi}(t)} - (\mu_{hi}^\alpha + \delta_{hi}^\alpha + \gamma_{hi}^\alpha)I_{hi}(t), \\ F_k(t, R_{hi}(t)) &= \gamma_{ai}^\alpha A_{hi}(t) - (\mu_{hi}^\alpha + \gamma_{ui}^\alpha)R_{hi}(t), \\ F_k(t, A_{hi}(t)) &= (1 - \rho_h^\alpha)\gamma_{ei}^\alpha E_{hi}(t) - \frac{\rho_i^\alpha \beta_h^\alpha A_{hi}(t)I_v(t)}{N_{hi}(t)} + (1 - \theta_h^\alpha)\gamma_{hi}^\alpha I_{hi}(t) - \gamma_{ai}^\alpha A_{hi}(t) \\ &\quad - \mu_{hi}^\alpha A_{hi}(t), \\ F_k(t, S_v(t)) &= \Lambda_v^\alpha - \frac{\beta_v^\alpha S_v(t)(I_{hi}(t) + \sigma_i^\alpha A_{hi})}{N_{hi}} - \frac{(1 - \epsilon_h)\beta_v^\alpha S_v(t)(I_{hj}(t) + \sigma_j^\alpha A_{hj})}{N_{hj}} \\ &\quad - \mu_v^\alpha S_v(t), \\ F_k(t, E_v(t)) &= \frac{\beta_v^\alpha S_v(t)(I_{hi}(t) + \sigma_i^\alpha A_{hi})}{N_{hi}} + \frac{(1 - \epsilon_h)\beta_v^\alpha S_v(t)(I_{hj}(t) + \sigma_j^\alpha A_{hj})}{N_{hj}} \\ F_k(t, I_v(t)) &= \frac{-(\mu_v^\alpha + \gamma_v^\alpha)E_v(t)}{\gamma_v^\alpha E_v(t) - \mu_v^\alpha I_v(t)}. \end{aligned} \right\} \tag{2.8}$$

The kernels  $N_i$  with  $0 \leq Q_k < 1, i = 1, 2, \dots, 13$ , satisfy the Lipschitz condition in equation (2.8) if and only if  $S_{hi}(t), E_{hi}(t), I_{hi}(t), R_{hi}(t), A_{hi}(t), S_v(t), E_v(t)$ , and  $I_v(t)$ , with  $i = 1, 2$  have an upper bound. In-general, suppose  $S_{hi}(t)$  and  $S_{hi}^*(t)$  are two functions, we have:

$$\left. \begin{aligned} \|F_k t, S_{hi}(t) - F_k(t, S_{hi}^*(t))\| &= \left\| \Lambda_{hi}^\alpha - \frac{\beta_h^\alpha S_{hi}(t)I_v(t)}{N_{hi}(t)} - \mu_{hi}^\alpha S_{hi}(t) - p_{hi}^\alpha S_{hi}(t) + p_{hj}^\alpha S_{hj}(t) \right. \\ &\quad \left. + \gamma_{ui}^\alpha R_{hi}(t) + \theta_{hi}^\alpha \gamma_{hi}^\alpha I_{hi}(t) - \left( \Lambda_{hi}^\alpha - \frac{\beta_h^\alpha S_{hi}^*(t)I_v(t)}{N_{hi}(t)} - \mu_{hi}^\alpha S_{hi}^*(t) \right) \right. \\ &\quad \left. - p_{hi}^\alpha S_{hi}^*(t) + p_{hj}^\alpha S_{hj}^*(t) + \gamma_{ui}^\alpha R_{hi}(t) + \theta_{hi}^\alpha \gamma_{hi}^\alpha I_{hi}(t) \right\|, \\ &= \left( \frac{\beta_h^\alpha I_{hi}}{N_{hi}} + \mu_h^\alpha + p_{hi}^\alpha \right) \|S_{hi} - S_{hi}^*\|, \\ &\leq \left( \frac{\beta_h^\alpha \sup_{t \in [0, T]} I_{hi}(t)}{\sup_{t \in [0, T]} N_{hi}(t)} + \mu_h^\alpha + p_{hi}^\alpha \right) \|S_{hi} - S_{hi}^*\|, \\ &= Q_k \|S_{hi} - S_{hi}^*\|. \end{aligned} \right\} \tag{2.9}$$

Where  $Q_k = \frac{\beta_h^\alpha \sup_{t \in [0, T]} I_{hi}(t)}{\sup_{t \in [0, T]} N_{hi}(t)} + \mu_h^\alpha + p_{hi}^\alpha$ . Thus:

$$\|F_k t, S_{hi}(t) - F_k(t, S_{hi}^*(t))\| \leq Q_k \|S_{hi} - S_{hi}^*\| \tag{2.10}$$

Using the same techniques as in (2.9), we get:

$$\left. \begin{aligned} \|F_k t, E_{hi}(t) - F_k(t, E_{hi}^*(t))\| &\leq Q_k \|E_{hi} - E_{hi}^*\|, \\ \|F_k t, I_{hi}(t) - F_k(t, I_{hi}^*(t))\| &\leq Q_k \|I_{hi} - I_{hi}^*\|, \\ \|F_k t, R_{hi}(t) - F_k(t, R_{hi}^*(t))\| &\leq Q_k \|R_{hi} - R_{hi}^*\|, \\ \|F_k t, A_{hi}(t) - F_k(t, A_{hi}^*(t))\| &\leq Q_k \|A_{hi} - A_{hi}^*\|, \\ \|F_k t, S_v(t) - F_k(t, S_v^*(t))\| &\leq Q_k \|S_v - S_v^*\|, \\ \|F_k t, E_v(t) - F_k(t, E_v^*(t))\| &\leq Q_k \|E_v - E_v^*\|, \\ \|F_k t, I_v(t) - F_k(t, I_v^*(t))\| &\leq Q_k \|I_v - I_v^*\|. \end{aligned} \right\} \tag{2.11}$$

Whereby  $Q_i (i = 1, 2, \dots, 12)$  is the Lipschitz constant for the function  $F_i(\cdot)$  for  $i = 1, 2, \dots, 12$ . Indeed, equation (2.7) in recursive form as follows:

$$\left. \begin{aligned} S_{hi}(t) &= S_{hi}(0) + \frac{(1-\alpha)}{M(\alpha)} F_k(t, S_{hi,n-1}(t)) + \frac{\alpha}{M(\alpha)} \frac{1}{\Gamma(\alpha)} \int_0^t (t-\tau)^{\alpha-1} F_k(\tau, S_{hi,n-1}(\tau)) d\tau, \\ E_{hi}(t) &= E_{hi}(0) + \frac{(1-\alpha)}{M(\alpha)} F_k(t, E_{hi,n-1}(t)) + \frac{\alpha}{M(\alpha)} \frac{1}{\Gamma(\alpha)} \int_0^t (t-\tau)^{\alpha-1} F_k(\tau, E_{hi,n-1}(\tau)) d\tau, \\ I_{hi}(t) &= I_{hi}(0) + \frac{(1-\alpha)}{M(\alpha)} F_k(t, I_{hi,n-1}(t)) + \frac{\alpha}{M(\alpha)} \frac{1}{\Gamma(\alpha)} \int_0^t (t-\tau)^{\alpha-1} F_k(\tau, I_{hi,n-1}(\tau)) d\tau, \\ A_{hi}(t) &= A_{hi}(0) + \frac{(1-\alpha)}{M(\alpha)} F_k(t, A_{hi,n-1}(t)) + \frac{\alpha}{M(\alpha)} \frac{1}{\Gamma(\alpha)} \int_0^t (t-\tau)^{\alpha-1} F_k(\tau, A_{hi,n-1}(\tau)) d\tau, \\ R_{hi}(t) &= R_{hi}(0) + \frac{(1-\alpha)}{M(\alpha)} F_k(t, R_{hi,n-1}(t)) + \frac{\alpha}{M(\alpha)} \frac{1}{\Gamma(\alpha)} \int_0^t (t-\tau)^{\alpha-1} F_k(\tau, R_{hi,n-1}(\tau)) d\tau, \end{aligned} \right\} \quad (2.12)$$

$$\left. \begin{aligned} S_v(t) &= S_v(0) + \frac{(1-\alpha)}{M(\alpha)} F_k(t, S_{v,n-1}(t)) + \frac{\alpha}{M(\alpha)} \frac{1}{\Gamma(\alpha)} \int_0^t (t-\tau)^{\alpha-1} F_k(\tau, S_{v,n-1}(\tau)) d\tau, \\ E_v(t) &= E_v(0) + \frac{(1-\alpha)}{M(\alpha)} F_k(t, E_{v,n-1}(t)) + \frac{\alpha}{M(\alpha)} \frac{1}{\Gamma(\alpha)} \int_0^t (t-\tau)^{\alpha-1} F_k(\tau, E_{v,n-1}(\tau)) d\tau, \\ I_v(t) &= I_v(0) + \frac{(1-\alpha)}{M(\alpha)} F_k(t, I_{v,n-1}(t)) + \frac{\alpha}{M(\alpha)} \frac{1}{\Gamma(\alpha)} \int_0^t (t-\tau)^{\alpha-1} F_k(\tau, I_{v,n-1}(\tau)) d\tau. \end{aligned} \right\} \quad (2.13)$$

Suppose  $\Psi_k, k = 1, 2, \dots, 13$  be the difference between successive components in (2.12) and (2.13). We have the following:

$$\left. \begin{aligned} \Psi_n^k &= S_{hi,n}(t) - S_{hi,n-1}(t) = \frac{1-\alpha}{M(\alpha)} (F_k(t, S_{hi,n-1}(t)) - F_k(t, S_{hi,n-2}(t))) \\ &\quad + \frac{\alpha}{M(\alpha)} \frac{1}{\Gamma(\alpha)} \int_0^t (t-\tau)^{\alpha-1} (F_k(\tau, S_{hi,n-1}(\tau)) - F_k(\tau, S_{hi,n-2}(\tau))) d\tau, \\ \Psi_n^k &= E_{hi,n}(t) - E_{hi,n-1}(t) = \frac{1-\alpha}{M(\alpha)} (F_k(t, E_{hi,n-1}(t)) - F_k(t, E_{hi,n-2}(t))) \\ &\quad + \frac{\alpha}{M(\alpha)} \frac{1}{\Gamma(\alpha)} \int_0^t (t-\tau)^{\alpha-1} (F_k(\tau, E_{hi,n-1}(\tau)) - F_k(\tau, E_{hi,n-2}(\tau))) d\tau, \\ \Psi_n^k &= I_{hi,n}(t) - I_{hi,n-1}(t) = \frac{1-\alpha}{M(\alpha)} (F_k(t, I_{hi,n-1}(t)) - F_k(t, I_{hi,n-2}(t))) \\ &\quad + \frac{\alpha}{M(\alpha)} \frac{1}{\Gamma(\alpha)} \int_0^t (t-\tau)^{\alpha-1} (F_k(\tau, I_{hi,n-1}(\tau)) - F_k(\tau, I_{hi,n-2}(\tau))) d\tau, \\ \Psi_n^k &= A_{hi,n}(t) - A_{hi,n-1}(t) = \frac{1-\alpha}{M(\alpha)} (F_k(t, A_{hi,n-1}(t)) - F_k(t, A_{hi,n-2}(t))) \\ &\quad + \frac{\alpha}{M(\alpha)} \frac{1}{\Gamma(\alpha)} \int_0^t (t-\tau)^{\alpha-1} (F_k(\tau, A_{hi,n-1}(\tau)) - F_k(\tau, A_{hi,n-2}(\tau))) d\tau, \\ \Psi_n^k &= R_{hi,n}(t) - R_{hi,n-1}(t) = \frac{1-\alpha}{M(\alpha)} (F_k(t, R_{hi,n-1}(t)) - F_k(t, R_{hi,n-2}(t))) \\ &\quad + \frac{\alpha}{M(\alpha)} \frac{1}{\Gamma(\alpha)} \int_0^t (t-\tau)^{\alpha-1} (F_k(\tau, R_{hi,n-1}(\tau)) - F_k(\tau, R_{hi,n-2}(\tau))) d\tau, \\ \Psi_n^k &= S_{v,n}(t) - S_{v,n-1}(t) = \frac{1-\alpha}{M(\alpha)} (F_k(t, S_{v,n-1}(t)) - F_k(t, S_{v,n-2}(t))) \\ &\quad + \frac{\alpha}{M(\alpha)} \frac{1}{\Gamma(\alpha)} \int_0^t (t-\tau)^{\alpha-1} (F_k(\tau, S_{v,n-1}(\tau)) - F_k(\tau, S_{v,n-2}(\tau))) d\tau, \\ \Psi_n^k &= E_{v,n}(t) - E_{v,n-1}(t) = \frac{1-\alpha}{M(\alpha)} (F_k(t, E_{v,n-1}(t)) - F_k(t, E_{v,n-2}(t))) \\ &\quad + \frac{\alpha}{M(\alpha)} \frac{1}{\Gamma(\alpha)} \int_0^t (t-\tau)^{\alpha-1} (F_k(\tau, E_{v,n-1}(\tau)) - F_k(\tau, E_{v,n-2}(\tau))) d\tau, \\ \Psi_n^k &= I_{v,n}(t) - I_{v,n-1}(t) = \frac{1-\alpha}{M(\alpha)} (F_k(t, I_{v,n-1}(t)) - F_k(t, I_{v,n-2}(t))) \\ &\quad + \frac{\alpha}{M(\alpha)} \frac{1}{\Gamma(\alpha)} \int_0^t (t-\tau)^{\alpha-1} (F_k(\tau, I_{v,n-1}(\tau)) - F_k(\tau, I_{v,n-2}(\tau))) d\tau. \end{aligned} \right\} \quad (2.14)$$

Considering that  $S_{hi,n}(t) = \sum_{r=1}^n \Psi_r^k(t), E_{hi,n}(t) = \sum_{r=1}^n \Psi_r^k(t), I_{hi,n}(t) = \sum_{r=1}^n \Psi_r^k(t), A_{hi,n}(t) = \sum_{r=1}^n \Psi_r^k(t), R_{hi,n}(t) = \sum_{r=1}^n \Psi_r^k(t), S_{v,n}(t) = \sum_{r=1}^n \Psi_r^k(t), E_{v,n}(t) = \sum_{r=1}^n \Psi_r^k(t),$  and  $I_{v,n}(t) = \sum_{r=1}^n \Psi_r^k(t).$

Taking the norm on both sides of the equation and using equations (2.14) and (2.10), we have:

$$\|\Psi_n^k(t)\| = \frac{1-\alpha}{M(\alpha)} Q_k \|\Psi_{n-1}^k(t)\| + \frac{\alpha}{M(\alpha)} \frac{Q_k}{\Gamma(\alpha)} \int_0^t (t-\tau)^{\alpha-1} \|\Psi_{n-1}^k(\tau)\| d\tau, \quad (2.15)$$

In what follows, we state and prove the following theorem based on the results in (2.15).

**Theorem 3.** *The model system (2.1) has a unique solution for  $t \in [0, T]$  if the condition below satisfies.*

$$\left(\frac{1-\alpha}{M(\alpha)}Q_k + \frac{1}{M(\alpha)}\frac{Q_k}{\Gamma(\alpha)}T^\alpha\right), \quad k = 1, 2, \dots, 13 \tag{2.16}$$

Since the function  $S_{hi}(t)$ ,  $E_{hi}(t)$ ,  $I_{hi}(t)$ ,  $A_{hi}(t)$ ,  $R_{hi}(t)$ ,  $S_v(t)$ ,  $E_v(t)$  and  $I_v(t)$  are bounded and satisfy the Lipschitz condition, and using (2.16), we have:

$$\left. \begin{aligned} \|Q_n^k(t)\| &\leq \|S_{hi,n}(0)\| \left(\frac{1-\alpha}{M(\alpha)}Q_k + \frac{1}{M(\alpha)}\frac{Q_k}{\Gamma(\alpha)}T^\alpha\right)^n, \\ \|Q_n^k(t)\| &\leq \|E_{hi,n}(0)\| \left(\frac{1-\alpha}{M(\alpha)}Q_k + \frac{1}{M(\alpha)}\frac{Q_k}{\Gamma(\alpha)}T^\alpha\right)^n, \\ \|Q_n^k(t)\| &\leq \|I_{hi,n}(0)\| \left(\frac{1-\alpha}{M(\alpha)}Q_k + \frac{1}{M(\alpha)}\frac{Q_k}{\Gamma(\alpha)}T^\alpha\right)^n, \\ \|Q_n^k(t)\| &\leq \|A_{hi,n}(0)\| \left(\frac{1-\alpha}{M(\alpha)}Q_k + \frac{1}{M(\alpha)}\frac{Q_k}{\Gamma(\alpha)}T^\alpha\right)^n, \\ \|Q_n^k(t)\| &\leq \|R_{hi,n}(0)\| \left(\frac{1-\alpha}{M(\alpha)}Q_k + \frac{1}{M(\alpha)}\frac{Q_k}{\Gamma(\alpha)}T^\alpha\right)^n, \\ \|Q_n^k(t)\| &\leq \|S_{v,n}(0)\| \left(\frac{1-\alpha}{M(\alpha)}Q_k + \frac{1}{M(\alpha)}\frac{Q_{11}}{\Gamma(\alpha)}T^\alpha\right)^n, \\ \|Q_n^k(t)\| &\leq \|E_{v,n}(0)\| \left(\frac{1-\alpha}{M(\alpha)}Q_k + \frac{1}{M(\alpha)}\frac{Q_k}{\Gamma(\alpha)}T^\alpha\right)^n, \\ \|Q_n^k(t)\| &\leq \|I_{v,n}(0)\| \left(\frac{1-\alpha}{M(\alpha)}Q_k + \frac{1}{M(\alpha)}\frac{Q_k}{\Gamma(\alpha)}T^\alpha\right)^n. \end{aligned} \right\} \tag{2.17}$$

Therefore, the sequence in (2.17) exist, and  $\|Q_n^k\| \rightarrow 0$  as  $n \rightarrow \infty$ ,  $k = 1, 2, \dots, 13$ . In addition, using the triangular inequality in (2.17), for any  $s$  we have:

$$\left. \begin{aligned} \|S_{hi,n+s} - S_{hi,n}\| &\leq \sum_{r=n+1}^{n+s} q_k^r = \frac{q_1^{n+1} - q_k^{n+s+1}}{1 - q_k}, \\ \|E_{hi,n+s} - E_{hi,n}\| &\leq \sum_{r=n+1}^{n+s} q_k^r = \frac{q_k^{n+1} - q_k^{n+s+1}}{1 - q_k}, \\ \|I_{hi,n+s} - I_{hi,n}\| &\leq \sum_{r=n+1}^{n+s} q_k^r = \frac{q_k^{n+1} - q_k^{n+s+1}}{1 - q_5}, \\ \|A_{hi,n+s} - A_{hi,n}\| &\leq \sum_{r=n+1}^{n+s} q_7^r = \frac{q_k^{n+1} - q_k^{n+s+1}}{1 - q_k}, \\ \|R_{hi,n+s} - R_{hi,n}\| &\leq \sum_{r=n+1}^{n+s} q_9^r = \frac{q_k^{n+1} - q_k^{n+s+1}}{1 - q_k}, \\ \|S_{v,n+s} - S_{v,n}\| &\leq \sum_{r=n+1}^{n+s} q_{11}^r = \frac{q_k^{n+1} - q_k^{n+s+1}}{1 - q_k}, \\ \|E_{v,n+s} - E_{v,n}\| &\leq \sum_{r=n+1}^{n+s} q_k^r = \frac{q_k^{n+1} - q_k^{n+s+1}}{1 - q_k}, \\ \|I_{v,n+s} - I_{v,n}\| &\leq \sum_{r=n+1}^{n+s} q_{13}^r = \frac{q_k^{n+1} - q_k^{n+s+1}}{1 - q_k}. \end{aligned} \right\} \tag{2.18}$$

Where  $q_k$ ,  $k = 1, 2, \dots, 13$  are the terms inside the brackets in (2.17). Thus,  $S_{hi}(t)$ ,  $E_{hi}(t)$ ,  $I_{hi}(t)$ ,  $A_{hi}(t)$ ,  $R_{hi}(t)$ ,  $S_v(t)$ ,  $E_v(t)$  and  $I_v(t)$ ,  $i = 1, 2$  are the Cauchy sequences in  $\mathcal{B}$ . Therefore, one can note that as  $n \rightarrow \infty$  in (2.13), the limit of these sequences is the unique solution of the model system (2.1). This completes the proofs of unique solution of the system (2.1).

### 2.5 Euler approximation scheme of model (2.1) using Atangana-Baleanu-Caputo derivative sense

Here, we discuss the an efficient of numerical scheme called Euler fractional approximation method for proposed model (2.1) in the sense of Atangana-Baleanu-Caputo fractional derivatives as used in

[58]. The proposed model differential equation equations can be presented in the following form:

$$\left. \begin{aligned} {}^{ABC}D_0^\alpha S_{hi}(t) &= G_1(t, S_{hi}) \\ {}^{ABC}D_0^\alpha E_{hi}(t) &= G_2(t, E_{hi}) \\ {}^{ABC}D_0^\alpha I_{hi}(t) &= G_3(t, I_{hi}) \\ {}^{ABC}D_0^\alpha A_{hi}(t) &= G_4(t, S_{hi}) \\ {}^{ABC}D_0^\alpha R_{hi}(t) &= G_5(t, R_{hi}) \\ {}^{ABC}D_0^\alpha S_v(t) &= G_6(t, S_v) \\ {}^{ABC}D_0^\alpha E_v(t) &= G_7(t, E_v) \\ {}^{ABC}D_0^\alpha I_v(t) &= G_8(t, I_v) \end{aligned} \right\} \quad (2.19)$$

In what follows, we represent equation (2.19) for  $G_1(t, S_{hi})$  which satisfies the Lipschitz condition and the  $S_{hi}(0)$  is the initial conditions. Now applying the non-integer operator to equation (2.19) we have that:

$$S_{hi}(t) = S_{hi}(0) + {}^{ABC}I_0^\alpha G_1(t, S_{hi}) \quad (2.20)$$

Where  ${}^{ABC}I_0^\alpha$  represent the fractional integer operator with respect to the ABC fractional derivatives. For the proposed numerical method, we consider an interval length  $[0, d]$  with time step size  $h = \frac{d}{N}$  where  $N \in \mathbb{N}$ . Let  $S_{hi_k}$  be the numerical approximation of  $S_{hi}(t)$  at  $t = t_k$ , where  $t_k = 0 + kh$  and  $k = 0, 1, 2, 3, \dots, N$ . Applying Euler method in (2.20), we have the following ABC operator formula:

$$S_{hi_{k+1}}(t) = S_{hi}(0) + \frac{1-\alpha}{M(\alpha)} G_1(S_{hi_{k+1}}) + \frac{h^\alpha}{M(\alpha)\Gamma(\alpha)} \sum_{p=0}^k z_{k+1,p} G_1(S_{hi_p}), \quad k = 0, 1, 2, \dots, N-1 \quad (2.21)$$

Where  $z_{k+1,p} = (k+1-p)^\alpha - (k-p)^\alpha, p = 0, 1, \dots, k$ . The stability analysis of the proposed model is given by the following theorem:

**Theorem 4.** *The numerical approximation scheme (2.21) is conditionally stable*

*Proof.* Let  $\tilde{S}_{hi_0}$  and  $\tilde{S}_{hi_p}$  be approximations of  $S_{hi_0}$  and  $S_{hi_p}, p = 0, \dots, k+1$ . From equation (2.21) we have:

$$S_{hi_{k+1}} + \tilde{S}_{hi_{k+1}} = S_{hi_0} + \tilde{S}_{hi_0} + \frac{1-\alpha}{M(\alpha)} G_1(S_{hi_{k+1}} + \tilde{S}_{hi_{k+1}}) + \frac{h^\alpha}{M(\alpha)\Gamma(\alpha)} \sum_{p=0}^k z_{k+1,p} G_1(S_{hi_p} + \tilde{S}_{hi_p}) \quad (2.22)$$

Using equation (2.21) in (2.22), we get:

$$|\tilde{S}_{hi_{k+1}}| = |S_{hi_0} + \frac{1-\alpha}{M(\alpha)} [G_1(S_{hi_{k+1}} + \tilde{S}_{hi_{k+1}}) - G_1(S_{hi_{k+1}})] + \frac{h^\alpha}{M(\alpha)\Gamma(\alpha+1)} \sum_{p=0}^k z_{k+1,p} [G_1(S_{hi_p} + \tilde{S}_{hi_p}) - G_1(S_{hi_p})]| \quad (2.23)$$

Applying the Lipschitz condition and triangular inequality, one get the following:

$$|\tilde{S}_{hi_{k+1}}| \leq \epsilon_0 + \frac{(1-\alpha)V_1}{M(\alpha)} |\tilde{S}_{hi_{k+1}}| + \frac{\alpha h^\alpha V_1}{M(\alpha)\Gamma(\alpha+1)} \sum_{p=0}^k z_{k+1,p} |\tilde{S}_{hi_p}| \quad (2.24)$$

Where  $\epsilon_0 = \max_{0 \leq k \leq N} \{|\tilde{S}_{hi_0}| + \frac{\alpha h^\alpha V_1 z_{k,0}}{M(\alpha)\Gamma(\alpha+1)} |\tilde{S}_{hi_0}|\}$  Equation (2.24) can be further simplified and we get the following:

$$|\tilde{S}_{hi_{k+1}}| \leq V_1 V_{1\alpha} \epsilon_0 + \frac{\alpha h^\alpha V_1 V_{1\alpha}}{M(\alpha)\Gamma(\alpha+1)} \sum_{p=0}^k z_{k+1,p} |\tilde{S}_{hi_p}| \quad (2.25)$$

Where  $V_{1\alpha} = \frac{M(\alpha)}{|(\alpha-1)V_1 + M(\alpha)|}$ . Finally we have that  $|\tilde{S}_{hi_{k+1}}| \leq CV_{1\alpha} \epsilon_0$  and this complete the proof.  $\square$

### 3 Numerical Simulations

In this section, we use the MATLAB programming language to perform the numerical simulation of the model system (2.1) to gain insight into the behavior of the solution for fractional-order

derivatives. We utilized the fractional Adam-Bashforth-Moulton scheme to simulate the model (2.1) as illustrated below;

Consider the nonlinear differential equation:

$${}^c D_t^\alpha \Phi(t) = f(t, \Phi(t)), 0 \leq t \leq T \tag{3.1}$$

With the initial conditions:

$$\Phi^p(t) = \Phi_0^p, \quad p = 0, 1, 2, \dots, [q] - 1 \tag{3.2}$$

Now, with operating by the fractional integral operator on the equation (3.1), we can obtain on the solution  $\Phi(t)$  by solving the following equation:

$$\Phi^\alpha(t) = \sum_{p=0}^{|\alpha|-1} \frac{\Phi_0^p}{p!} t^p + \frac{1}{\Gamma(\alpha)} \int_0^t (t-\tau)^{\alpha-1} f(\tau, \Phi(\tau)) d\tau \tag{3.3}$$

Diethelm [45] used the predictor-corrector scheme based on the Adam-Bashforth-Moulton algorithm to solve the equation 3.1. setting  $h = \frac{T}{N}$ ,  $t_n = nh$  and  $n = 0, 1, 2, \dots, N \in \mathbb{Z}^+$ . Therefore we can discretize the equation (3.1) as follows:

$$\Phi_h(t_{n+1}) = \sum_{p=0}^{|\alpha|-1} \frac{\Phi_0^p}{p!} t_{n+1}^p + \frac{h^\alpha}{\Gamma(\alpha+2)} \sum_{m=0}^n a_{m,n+1} f(t_m, \Phi_m) + \frac{h^\alpha}{\Gamma(\alpha+2)} f(t_{n+1}, \Phi_{n+1}^v) \tag{3.4}$$

where Where by  $t_m = mh$  with some fixed  $h$  and:

$$a_{m,n+1} = \begin{cases} n^{\alpha+1} - (n-\alpha)(n+\alpha)^\alpha, & m = 0, \\ (n-m+2)^{\alpha+1} + (n-m)^{\alpha+1} - 2(n-m+1)^{\alpha+1}, & 1 \leq m \leq n, \\ 1 & \text{if } m = n+1. \end{cases}$$

and the predicted value :

$$\Phi_{t_{n+1}}^p = \sum_{p=0}^{|\alpha|-1} \frac{\Phi_0^p}{p!} t_{n+1}^p + \frac{1}{\Gamma(\alpha)} \sum_{m=0}^n b_{m,n+1} f(t_m, \Phi_h(t_m)) \tag{3.5}$$

With

$$b_{m,n+1} = \frac{h^\alpha}{\alpha} \left( (n+1-m)^\alpha - (n-m)^\alpha \right) \tag{3.6}$$

The error estimate is

$$\max_{0 \leq m \leq k} |\Phi(t_m) - \Phi_h(t_m)| = O(h^p) \tag{3.7}$$

with  $k \in \mathbb{N}$  and  $p = \min(2, n + \alpha)$

### 3.1 Application of Adam-Bashforth-Moulton Scheme to the proposed model

In this section, we utilize the Adam-Bashforth-Moulton method to numerically solve the nonlinear fractional-order model (2.1). In the view to the generalized Adam-Bashforth-Moulton scheme, the

proposed model (2.1) has the following form:

$$\left. \begin{aligned}
 S_{hi}(t_{n+1}) &= S_{hi}^0 + \frac{h^\alpha}{\Gamma(\alpha+2)} f_{S_{hi}}(t_{n+1}, S_{hi}^p(t_{n+1}), E_{hi}^p(t_{n+1}), I_{hi}^p(t_{n+1}), A_{hi}^p(t_{n+1}), \\
 &\quad R_{hi}^p(t_{n+1}), S_v^p(t_{n+1}), E_v^p(t_{n+1}), I_v^p(t_{n+1})) \\
 &\quad + \frac{h^\alpha}{\Gamma(\alpha+2)} \sum_{m=0}^n a_{m,n+1} f_{S_{hi}}(t_m, S_{hi}(t_m), E_{hi}(t_m), I_{hi}(t_m), A_{hi}(t_m), \\
 &\quad R_{hi}(t_m), S_v(t_m), E_v(t_m), I_v(t_m)), \\
 E_{hi}(t_{n+1}) &= E_{hi}^0 + \frac{h^\alpha}{\Gamma(\alpha+2)} f_{E_{hi}}(t_{n+1}, S_{hi}^p(t_{n+1}), E_{hi}^p(t_{n+1}), I_{hi}^p(t_{n+1}), A_{hi}^p(t_{n+1}), \\
 &\quad R_{hi}(t_{n+1}), S_v(t_{n+1}), E_v(t_{n+1}), I_v(t_{n+1})) \\
 &\quad + \frac{h^\alpha}{\Gamma(\alpha+2)} \sum_{m=0}^n a_{m,n+1} f_{E_{hi}}(t_m, S_{hi}(t_m), E_{hi}(t_m), I_{hi}(t_m), A_{hi}(t_m), \\
 &\quad R_{hi}(t_m), S_v(t_m), E_v(t_m), I_v(t_m)), \\
 I_{hi}(t_{n+1}) &= I_{hi}^0 + \frac{h^\alpha}{\Gamma(\alpha+2)} f_{I_{hi}}(t_{n+1}, S_{hi}^p(t_{n+1}), E_{hi}^p(t_{n+1}), I_{hi}^p(t_{n+1}), A_{hi}^p(t_{n+1}), \\
 &\quad R_{hi}(t_{n+1}), S_v(t_{n+1}), E_v(t_{n+1}), I_v(t_{n+1})) \\
 &\quad + \frac{h^\alpha}{\Gamma(\alpha+2)} \sum_{m=0}^n a_{m,n+1} f_{I_{hi}}(t_m, S_{hi}(t_m), E_{hi}(t_m), I_{hi}(t_m), A_{hi}(t_m), \\
 &\quad R_{hi}(t_m), S_v(t_m), E_v(t_m), I_v(t_m)), \\
 A_{hi}(t_{n+1}) &= A_{hi}^0 + \frac{h^\alpha}{\Gamma(\alpha+2)} f_{A_{hi}}(t_{n+1}, S_{hi}^p(t_{n+1}), E_{hi}^p(t_{n+1}), I_{hi}^p(t_{n+1}), A_{hi}^p(t_{n+1}), \\
 &\quad R_{hi}(t_{n+1}), S_v(t_{n+1}), E_v(t_{n+1}), I_v(t_{n+1})) \\
 &\quad + \frac{h^\alpha}{\Gamma(\alpha+2)} \sum_{m=0}^n a_{m,n+1} f_{A_{hi}}(t_m, S_{hi}(t_m), E_{hi}(t_m), I_{hi}(t_m), A_{hi}(t_m), \\
 &\quad R_{hi}(t_m), S_v(t_m), E_v(t_m), I_v(t_m)).
 \end{aligned} \right\}$$
  

$$\left. \begin{aligned}
 R_{hi}(t_{n+1}) &= R_{hi}^0 + \frac{h^\alpha}{\Gamma(\alpha+2)} f_{R_{hi}}(t_{n+1}, S_{hi}^p(t_{n+1}), E_{hi}^p(t_{n+1}), I_{hi}^p(t_{n+1}), A_{hi}^p(t_{n+1}), \\
 &\quad R_{hi}(t_{n+1}), S_v(t_{n+1}), E_v(t_{n+1}), I_v(t_{n+1})) \\
 &\quad + \frac{h^\alpha}{\Gamma(\alpha+2)} \sum_{m=0}^n a_{m,n+1} f_{R_{hi}}(t_m, S_{hi}(t_m), E_{hi}(t_m), I_{hi}(t_m), A_{hi}(t_m), \\
 &\quad R_{hi}(t_m), S_v(t_m), E_v(t_m), I_v(t_m)), \\
 S_v(t_{n+1}) &= S_v^0 + \frac{h^\alpha}{\Gamma(\alpha+2)} f_{S_v}(t_{n+1}, S_{hi}^p(t_{n+1}), E_{hi}^p(t_{n+1}), I_{hi}^p(t_{n+1}), A_{hi}^p(t_{n+1}), \\
 &\quad R_{hi}(t_{n+1}), S_v(t_{n+1}), E_v(t_{n+1}), I_v(t_{n+1})) \\
 &\quad + \frac{h^\alpha}{\Gamma(\alpha+2)} \sum_{m=0}^n a_{m,n+1} f_{S_v}(t_m, S_{hi}(t_m), E_{hi}(t_m), I_{hi}(t_m), A_{hi}(t_m), \\
 &\quad R_{hi}(t_m), S_v(t_m), E_v(t_m), I_v(t_m)), \\
 E_v(t_{n+1}) &= E_v^0 + \frac{h^\alpha}{\Gamma(\alpha+2)} f_{E_v}(t_{n+1}, S_{hi}^p(t_{n+1}), E_{hi}^p(t_{n+1}), I_{hi}^p(t_{n+1}), A_{hi}^p(t_{n+1}), \\
 &\quad R_{hi}(t_{n+1}), S_v(t_{n+1}), E_v(t_{n+1}), I_v(t_{n+1})) \\
 &\quad + \frac{h^\alpha}{\Gamma(\alpha+2)} \sum_{m=0}^n a_{m,n+1} f_{E_v}(t_m, S_{hi}(t_m), E_{hi}(t_m), I_{hi}(t_m), A_{hi}(t_m), \\
 &\quad R_{hi}(t_m), S_v(t_m), E_v(t_m), I_v(t_m)), \\
 I_v(t_{n+1}) &= I_v^0 + \frac{h^\alpha}{\Gamma(\alpha+2)} f_{I_v}(t_{n+1}, S_{hi}^p(t_{n+1}), E_{hi}^p(t_{n+1}), I_{hi}^p(t_{n+1}), A_{hi}^p(t_{n+1}), \\
 &\quad R_{hi}(t_{n+1}), S_v(t_{n+1}), E_v(t_{n+1}), I_v(t_{n+1})) \\
 &\quad + \frac{h^\alpha}{\Gamma(\alpha+2)} \sum_{m=0}^n a_{m,n+1} f_{I_v}(t_m, S_{hi}(t_m), E_{hi}(t_m), I_{hi}(t_m), A_{hi}(t_m), \\
 &\quad R_{hi}(t_m), S_v(t_m), E_v(t_m), I_v(t_m)).
 \end{aligned} \right\} \tag{3.8}$$

Where

$$\left. \begin{aligned}
 S_{hi}^p(t_{n+1}) &= S_{hi}^0 + \frac{1}{\Gamma\alpha} \sum_{m=0}^n b_{m,n+1} f_{S_{hi}}(t_m, S_{hi}(t_m), E_{hi}(t_m), I_{hi}(t_m), A_{hi}(t_m), R_{hi}(t_m), S_v(t_m), E_v(t_m), I_v(t_m)), \\
 E_{hi}^p(t_{n+1}) &= E_{hi}^0 + \frac{1}{\Gamma\alpha} \sum_{m=0}^n b_{m,n+1} f_{E_{hi}}(t_m, S_{hi}(t_m), E_{hi}(t_m), I_{hi}(t_m), A_{hi}(t_m), R_{hi}(t_m), S_v(t_m), E_v(t_m), I_v(t_m)), \\
 I_{hi}^p(t_{n+1}) &= I_{hi}^0 + \frac{1}{\Gamma\alpha} \sum_{m=0}^n b_{m,n+1} f_{I_{hi}}(t_m, S_{hi}(t_m), E_{hi}(t_m), I_{hi}(t_m), A_{hi}(t_m), R_{hi}(t_m), S_v(t_m), E_v(t_m), I_v(t_m)), \\
 A_{hi}^p(t_{n+1}) &= A_{hi}^0 + \frac{1}{\Gamma\alpha} \sum_{m=0}^n b_{m,n+1} f_{A_{hi}}(t_m, S_{hi}(t_m), E_{hi}(t_m), I_{hi}(t_m), A_{hi}(t_m), R_{hi}(t_m), S_v(t_m), E_v(t_m), I_v(t_m)), \\
 R_{hi}^p(t_{n+1}) &= R_{hi}^0 + \frac{1}{\Gamma\alpha} \sum_{m=0}^n b_{m,n+1} f_{R_{hi}}(t_m, S_{hi}(t_m), E_{hi}(t_m), I_{hi}(t_m), A_{hi}(t_m), R_{hi}(t_m), S_v(t_m), E_v(t_m), I_v(t_m)), \\
 S_v^p(t_{n+1}) &= S_v^0 + \frac{1}{\Gamma\alpha} \sum_{m=0}^n b_{m,n+1} f_{S_v}(t_m, S_{hi}(t_m), E_{hi}(t_m), I_{hi}(t_m), A_{hi}(t_m), R_{hi}(t_m), S_v(t_m), E_v(t_m), I_v(t_m)), \\
 E_v^p(t_{n+1}) &= E_v^0 + \frac{1}{\Gamma\alpha} \sum_{m=0}^n b_{m,n+1} f_{E_v}(t_m, S_{hi}(t_m), E_{hi}(t_m), I_{hi}(t_m), A_{hi}(t_m), R_{hi}(t_m), S_v(t_m), E_v(t_m), I_v(t_m)), \\
 I_v^p(t_{n+1}) &= I_v^0 + \frac{1}{\Gamma\alpha} \sum_{m=0}^n b_{m,n+1} f_{I_v}(t_m, S_{hi}(t_m), E_{hi}(t_m), I_{hi}(t_m), A_{hi}(t_m), R_{hi}(t_m), S_v(t_m), E_v(t_m), I_v(t_m)).
 \end{aligned} \right\} (3.9)$$

In what follows we have:

$$\left. \begin{aligned}
 {}^{ABC}D_0^\alpha S_{hi}(t) &= f_{S_{hi}}(t, S_{hi}(t), E_{hi}(t), I_{hi}(t), A_{hi}(t), R_{hi}(t), S_v(t), E_v(t), I_v(t)) \\
 {}^{ABC}D_0^\alpha E_{hi}(t) &= f_{E_{hi}}(t, S_{hi}(t), E_{hi}(t), I_{hi}(t), A_{hi}(t), R_{hi}(t), S_v(t), E_v(t), I_v(t)) \\
 {}^{ABC}D_0^\alpha I_{hi}(t) &= f_{I_{hi}}(t, S_{hi}(t), E_{hi}(t), I_{hi}(t), A_{hi}(t), R_{hi}(t), S_v(t), E_v(t), I_v(t)) \\
 {}^{ABC}D_0^\alpha A_{hi}(t) &= f_{A_{hi}}(t, S_{hi}(t), E_{hi}(t), I_{hi}(t), A_{hi}(t), R_{hi}(t), S_v(t), E_v(t), I_v(t)) \\
 {}^{ABC}D_0^\alpha R_{hi}(t) &= f_{R_{hi}}(t, S_{hi}(t), E_{hi}(t), I_{hi}(t), A_{hi}(t), R_{hi}(t), S_v(t), E_v(t), I_v(t)), \\
 {}^{ABC}D_0^\alpha S_v(t) &= f_{S_v}(t, S_{hi}(t), E_{hi}(t), I_{hi}(t), A_{hi}(t), R_{hi}(t), S_v(t), E_v(t), I_v(t)) \\
 {}^{ABC}D_0^\alpha E_v(t) &= f_{E_v}(t, S_{hi}(t), E_{hi}(t), I_{hi}(t), A_{hi}(t), R_{hi}(t), S_v(t), E_v(t), I_v(t)) \\
 {}^{ABC}D_0^\alpha I_v(t) &= f_{I_v}(t, S_{hi}(t), E_{hi}(t), I_{hi}(t), A_{hi}(t), R_{hi}(t), S_v(t), E_v(t), I_v(t)).
 \end{aligned} \right\} (3.10)$$

Additionally, the quantities

$$\left. \begin{aligned}
 f_{S_{hi}}(t_{n+1}, S_{hi}^p(t_{n+1}), E_{hi}^p(t_{n+1}), I_{hi}^p(t_{n+1}), A_{hi}^p(t_{n+1}), R_{hi}^p(t_{n+1}), S_v^p(t_{n+1}), E_v^p(t_{n+1}), I_v^p(t_{n+1})), \\
 f_{E_{hi}}(t_{n+1}, S_{hi}^p(t_{n+1}), E_{hi}^p(t_{n+1}), I_{hi}^p(t_{n+1}), A_{hi}^p(t_{n+1}), R_{hi}^p(t_{n+1}), S_v^p(t_{n+1}), E_v^p(t_{n+1}), I_v^p(t_{n+1})), \\
 f_{I_{hi}}(t_{n+1}, S_{hi}^p(t_{n+1}), E_{hi}^p(t_{n+1}), I_{hi}^p(t_{n+1}), A_{hi}^p(t_{n+1}), R_{hi}^p(t_{n+1}), S_v^p(t_{n+1}), E_v^p(t_{n+1}), I_v^p(t_{n+1})), \\
 f_{A_{hi}}(t_{n+1}, S_{hi}^p(t_{n+1}), E_{hi}^p(t_{n+1}), I_{hi}^p(t_{n+1}), A_{hi}^p(t_{n+1}), R_{hi}^p(t_{n+1}), S_v^p(t_{n+1}), E_v^p(t_{n+1}), I_v^p(t_{n+1})), \\
 f_{R_{hi}}(t_{n+1}, S_{hi}^p(t_{n+1}), E_{hi}^p(t_{n+1}), I_{hi}^p(t_{n+1}), A_{hi}^p(t_{n+1}), R_{hi}^p(t_{n+1}), S_v^p(t_{n+1}), E_v^p(t_{n+1}), I_v^p(t_{n+1})), \\
 f_{S_v}(t_{n+1}, S_{hi}^p(t_{n+1}), E_{hi}^p(t_{n+1}), I_{hi}^p(t_{n+1}), A_{hi}^p(t_{n+1}), R_{hi}^p(t_{n+1}), S_v^p(t_{n+1}), E_v^p(t_{n+1}), I_v^p(t_{n+1})), \\
 f_{E_v}(t_{n+1}, S_{hi}^p(t_{n+1}), E_{hi}^p(t_{n+1}), I_{hi}^p(t_{n+1}), A_{hi}^p(t_{n+1}), R_{hi}^p(t_{n+1}), S_v^p(t_{n+1}), E_v^p(t_{n+1}), I_v^p(t_{n+1})), \\
 f_{I_v}(t_{n+1}, S_{hi}^p(t_{n+1}), E_{hi}^p(t_{n+1}), I_{hi}^p(t_{n+1}), A_{hi}^p(t_{n+1}), R_{hi}^p(t_{n+1}), S_v^p(t_{n+1}), E_v^p(t_{n+1}), I_v^p(t_{n+1})).
 \end{aligned} \right\} (3.11)$$



### 3.2 Sensitivity analysis of the reproduction number

The results from model system (2.1) have shown that the basic reproduction number is an important threshold parameter for persistence and extinction of cholera disease in the population. Most of the parameters in this study have been drawn from the literature as presented in Table 1 and some are estimated. Therefore, it important to perform the sensitivity analysis to demonstrate the influence of each parameter in the magnitude of basic reproduction number  $\mathcal{R}_0$ .

**Definition 3.** (See, [15]) The normalized sensitivity index of  $\mathcal{R}_0$  which depends on differentiability of parameter,  $\zeta$  is defined as follows:

$$\Phi_{\zeta}^{\mathcal{R}_0} = \frac{\partial \mathcal{R}_0}{\partial \zeta} \times \frac{\zeta}{\mathcal{R}_0} \tag{3.12}$$

The implication of the sensitivity analysis is that the model parameters whose sensitivity index is positive increase the magnitude of  $\mathcal{R}_0$  whenever they are increased and those with a negative index decrease the  $\mathcal{R}_0$  whenever they are increased. In what follows that, using (3.12), the value of normalized sensitivity index for each parameter used in the model (2.1) is summarized in Table 2.

**Table 1. Description of parameters used in the model system (2.1)**

Symbol	Description	Value	Units
$\Lambda_h$	New recruitment of human population	0.033	Day <sup>-1</sup> [42]
$\Lambda_v$	New recruitment of vector population	1000	Day <sup>-1</sup> [42]
$p_{h1}$	proportion of human movement from high to low risk areas	0.00002	Day <sup>-1</sup>
$p_{h2}$	proportion of human movement from low to high risk areas	0.00001	Day <sup>-1</sup>
$\mu_h$	Human population birth/natural death rate	0.0056	Day <sup>-1</sup> [?]
$\mu_v$	Vector population birth/ mortality rate of	0.033	Day <sup>-1</sup> [?]
$\gamma_u$	Rate at which temporary immune humans lose immunity	$\gamma_u = 0.03$	Day <sup>-1</sup> [46]
$d_h$	Disease mortality rate for humans	0.00009	Day <sup>-1</sup> [?]
$\gamma_v$	Rate at which exposed mosquito become infectious	0.091	Day <sup>-1</sup> [?]
$\gamma_e$	Rate at which exposed individuals become infectious	0.1	Day <sup>-1</sup> [?]
$\epsilon_h$	Reduction factor of disease infection in low risk areas	fitted	
$\kappa_h$	Incubation rate of human population	$\frac{1}{10}$	Day <sup>-1</sup> [?]
$\kappa_h$	Incubation rate of animal population	$\frac{1}{12}$	Day <sup>-1</sup> [?]
$\kappa_h$	Incubation rate of vector population	$\frac{1}{25}$	Day <sup>-1</sup> [?]
$\gamma_a$	Animal recovery rate	$\frac{1}{120}$	Day <sup>-1</sup> [?]
$\rho_h$	Progression rate individuals from asymptotic to infection class	0.03	Day <sup>-1</sup> [?]
$\theta_h$	Treatment rate of infected humans	fitted	
$\beta_h$	Infection rate for mosquito-to-susceptible human population	0.092	Day <sup>-1</sup> [?]
$\beta_v$	Infection rate for human-to-susceptible mosquito population	0.03	Day <sup>-1</sup> [?]
$\alpha_h$	Progression rate of individuals from exposed to infected class	fitted	

**Table 2. Sensitivity analysis of parameters for the model system (2.1)**

Parameter	$\Lambda_h$	$\Lambda_v$	$\mu_h$	$\mu_v$	$\beta_h$	$\beta_v$	$\rho_h$	$\gamma_h$
Index	-0.5	+0.5	+0.0023	-0.3926	+0.5348	+0.4652	+0.4652	-0.0228
Parameter	$\theta_h$	$\gamma_u$	$\gamma_a$	$\gamma_v$	$\alpha_h$	$p_{h1}$	$\epsilon_h$	
Index	-0.0035	+0.0968	-0.0592	+0.3919	+0.0263	-0.0083	-0.3297	

From the results in Fig. 1, it was noted that model parameters  $\Lambda_v$ ,  $\beta_h$ ,  $\beta_v$ ,  $\sigma$ ,  $\gamma_u$ ,  $\gamma_v$  and  $\alpha_h$  have the positive influence on the  $\mathcal{R}_0$ , that is, whenever they are increased, the magnitude of  $\mathcal{R}_0$  increases. For instance, an increase in  $\beta_h$  by 30% will lead to an increase in the magnitude of the  $\mathcal{R}_0$  by 53.48%. Model parameters with negative index values have a negative influence on  $\mathcal{R}_0$ , for example, an increase in vector mortality rate by  $\mu_v$  by 33% will lead to a decrease on magnitude of  $\mathcal{R}_0$  by 39.26%.

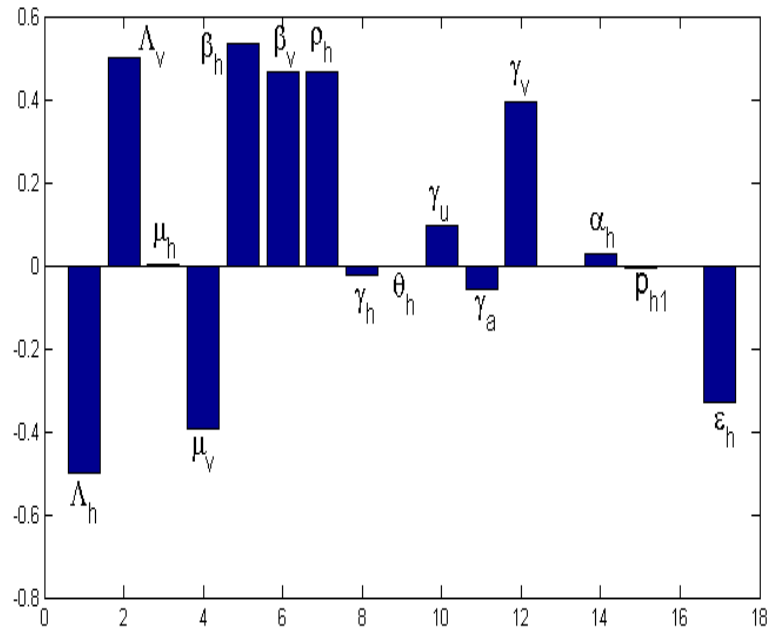


Fig. 1. Sensitivity analysis of the model system (2.1)

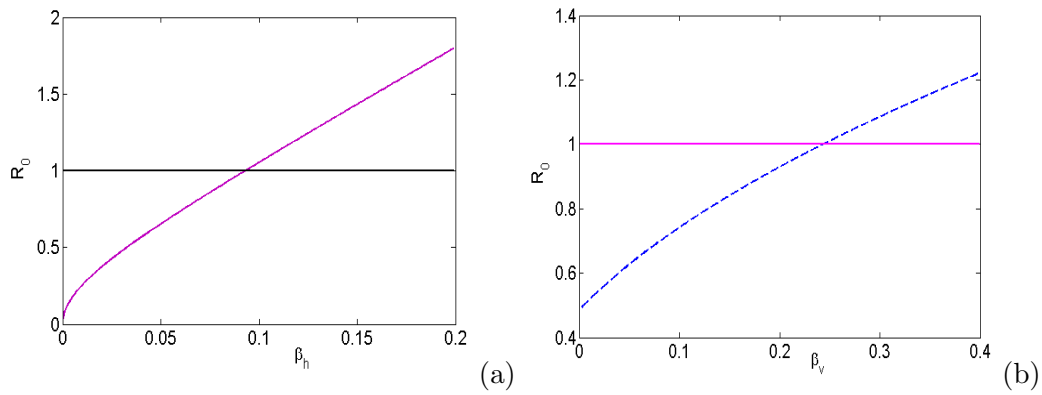
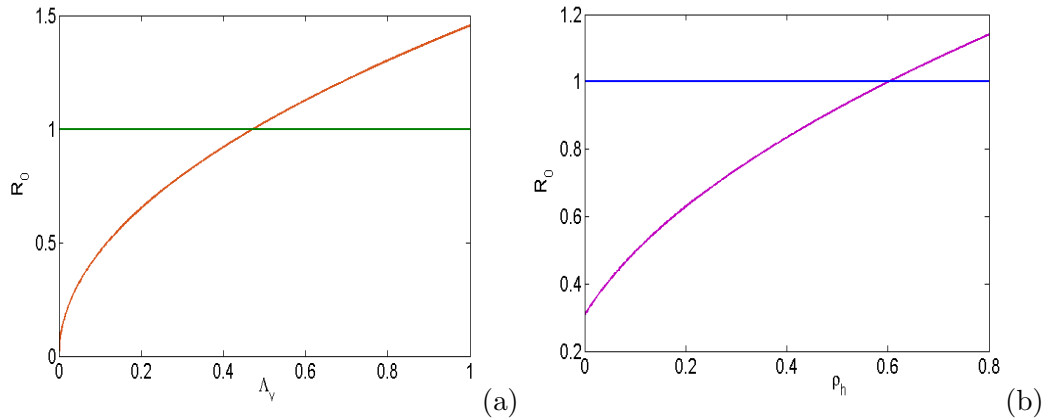


Fig. 2. Effects of varying (a) disease transmission rate from infected mosquitoes to susceptible humans modeled by parameter  $\beta_h$  on  $\mathcal{R}_0$  (b) disease transmission rate from infected humans to susceptible mosquitoes modeled by parameter  $\beta_v$  on  $\mathcal{R}_0$

Numerical results in Fig. 2. (a) shows the disease transmission rate from infected mosquitoes to susceptible humans modeled by parameter  $\beta_h$  on  $\mathcal{R}_0$ . From the results we note that increase on the disease transmission rate from infected mosquito to susceptible human increases the size of  $\mathcal{R}_0$ . In particular, whenever the transmission rate of disease from mosquitoes to humans in the population is greater than 10% the disease persists in the community. Fig. 2 (b) demonstrates the effect of disease transmission rate from infected humans to susceptible mosquitoes. Overall we observe

that whenever the transmission rate of disease from humans to mosquitoes is greater than 25% the disease can not be eliminated in the population. Simulations in Fig. 3 (a) depicts the effects of



**Fig. 3. Effects of varying (a) new recruitment of susceptible mosquitoes  $\beta_v$  on  $\mathcal{R}_0$  (b) progression rate of asymptotically humans to infectious class  $\rho_h$  on  $\mathcal{R}_0$**

varying new recruitment on susceptible mosquitoes  $\beta_v$  on  $\mathcal{R}_0$ . The results shows that increase in the new recruitment of susceptible mosquitoes increase the magnitude of  $\mathcal{R}_0$ . In particular, we can note that whenever  $\Lambda_v$  is greater than 50% the disease persists in the community. Fig. 2 (b) shows the effect of progression rate of asymptotically humans to infectious class. Overall we can note that whenever the  $\rho_h$  is greater than 60% the disease remain endemic in the community. Numerical

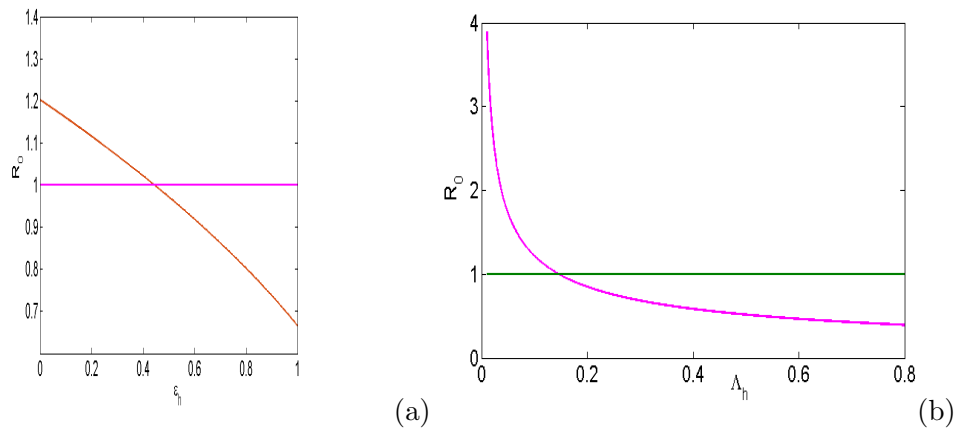


**Fig. 4. Effects of varying (a) reduction factor of disease transmission in low risk area  $\epsilon_h$  on  $\mathcal{R}_0$  (b) new recruitment of susceptible humans in the population  $\Lambda_h$  on  $\mathcal{R}_0$**

illustrations in Fig. 4 (a) shows the effect of varying reduction factor on the disease transmission in low risk area (modeled by the parameter  $\epsilon_h$ ) on  $\mathcal{R}_0$ . From the results we note that increase on the reduction factor decreases the size of  $\mathcal{R}_0$ . In particular, whenever  $\epsilon_h$  is greater than 50% the disease dies out in the population. Fig. 2. (b) shows the effect of varying the new recruitment of susceptible humans (modeled by the parameter  $\beta_h$ ) on  $\mathcal{R}_0$ . Overall we can note that whenever the  $\Lambda_h$  is greater than 20% the disease does not persist in the population. Fig. 5 shows the contour plot

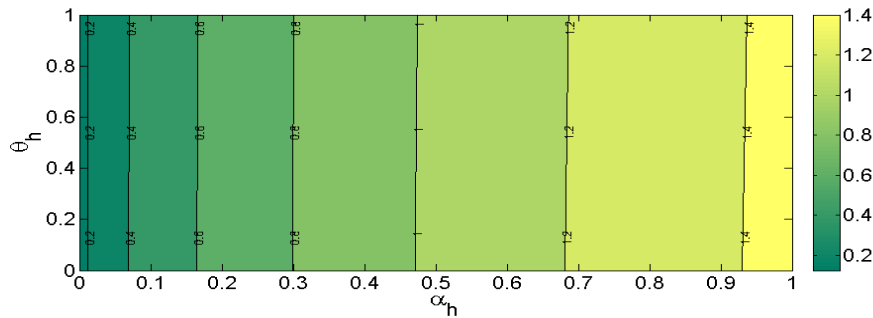


**Fig. 5. Contour plot of the basic reproduction number  $\mathcal{R}_0$  as the function of treatment rate on infected individuals (modeled by parameter  $\theta_h$ ) and progression rate of exposed humans to infectious class (modeled by parameter  $\alpha_h$ )**

of basic reproduction number  $\mathcal{R}_0$  as the function of treatment of infected individuals (modeled by parameter  $\theta_h$ ) and progression rate of exposed humans to infectious class (modeled by parameter  $\alpha_h$ ). Overall we can note that regardless of the treatment rate, increase on progression rate of exposed humans to infectious class by more than 50% in the population the malaria disease persists in the community.

### 3.3 Parameter estimations using weekly reports of malaria cases in Zimbabwe

In this section, we use the real data of Malaria cases reported in Zimbabwe to numerically solve the model system (2.1) and estimate the parameters  $(\epsilon_h, \theta_h, \alpha_h)$  that minimize the deviation of real data from prediction of model system (2.1). Fitting the model using real data and parameter estimation in the fractional order models is an integral part in the disease modeling. Therefore, in this study we use both the least squares and Nelder mead algorithm methods [7] to fit and estimate the parameters  $(\epsilon_h, \theta_h, \alpha_h)$  of the proposed model (2.1). The real data used in this study are weekly reported cases in Zimbabwe as presented in Table 3, and the commutative new infections predicted by the model (2.1) is obtained using the equation (3.13):

$${}^c D_t^q C(t) = \frac{\beta_h S_h(t) I_v(t)}{N_h(t)} \quad (3.13)$$

We use the following function to compute the best fitting:

$$\mathbb{F} : \mathbb{R}_{(\epsilon_h, \theta_h, \alpha_h)}^3 \rightarrow \mathbb{R}_{(\epsilon_h, \theta_h, \alpha_h)} \quad (3.14)$$

where  $\epsilon_h, \theta_h, \alpha_h$  are variables such that:

- (1) For a given  $(\epsilon_h, \theta_h, \alpha_h)$ , solve numerically the model differential equations (2.1) to obtain a solution  $\hat{Y}_i(t) = (\hat{S}_{hi}, \hat{E}_{hi}, \hat{I}_{hi}, \hat{A}_{hi}, \hat{R}_{hi}, \hat{S}_v, \hat{E}_v, \hat{I}_v)$  which is an approximation of the reported Malaria cases  $Y(t)$ .
- (2) Set  $t_0 = 1$  (the fitting process starts in week 1) and for  $t = 2, 3, \dots, 52$ , corresponding to weeks in where data are available, evaluate the computed numerical solution for  $I_h(t)$ ; that is.,  $\hat{I}_h(1), \hat{I}_h(2), \hat{I}_h(3), \dots, \hat{I}_h(52)$ .
- (3) Compute the root mean square (RMSE) of the difference between  $\hat{I}_h(1), \hat{I}_h(2), \dots, \hat{I}_h(52)$  and

observed cases. This function  $\mathbb{F}$  returns the root-mean-square error (RMSE) where

$$\text{RMSE} = \sqrt{\frac{1}{n} \sum_{k=1}^{52} (I_h(k) - \hat{I}_h(k))^2}, \tag{3.15}$$

- (4) Determine a global minimum for the RMSE using Nelder-Mead algorithm. The function  $\mathbb{F}$  takes values in  $\mathbb{R}^3$  and returns a positive real number. Using the formula (3.15), we computed the *RMSE* and was found to be 2.6571. This shows that the proposed model has deviations from observed real data. On performing the fitting process we assumed the following initial conditions  $S_{h1}(0) = 100, E_{h1}(0) = 90, I_{h1}(0) = 60, R_{h1}(0) = 20, A_{h1}(0) = 20, S_{h2}(0) = 800, E_{h2}(0) = 100, I_{h2}(0) = 100, R_{h2}(0) = 90, A_{h2}(0) = 10, S_v(0) = 115, E_v(0) = 50$  and  $I_v(0) = 36$  and the model parameters are in Table 1.

**Table 3. Commutative detected of malaria cases for 52 weeks in 2014 reported in Zimbabwe**

week	1	2	3	4	5	6	7	8	9	10	11	12
Cases	1381	1939	2567	2672	1114	2516	2714	2529	1767	1677	2157	2102
Week	13	14	15	16	17	18	19	20	21	22	23	24
Cases	1782	2466	3194	1801	2396	2592	3184	2139	2576	2936	2091	3365
Week	25	26	27	27	28	29	30	31	32	33	34	35
Cases	3957	3737	4820	3622	3742	3027	2938	4750	4238	4508	5204	4302
Week	36	37	38	39	41	42	43	44	45	46	47	48
Cases	3945	3723	4938	4008	4068	5130	4670	4640	3914	4051	668	2228
Week	49	50	51	52								
Cases	2638	2603	2409	2409								

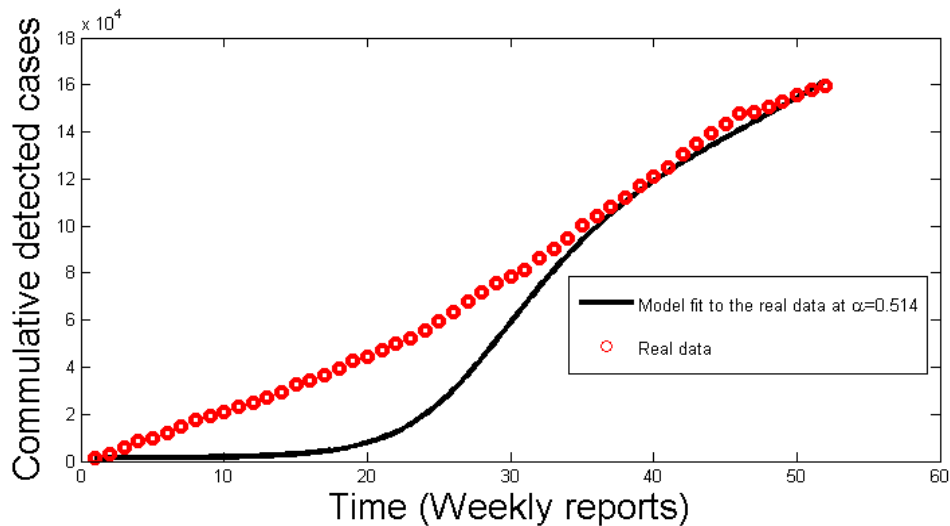


**Fig. 6. Estimation of the fractional-order model with  $\alpha = 0.514$  with RMSE=2.6557 with  $\mathcal{R}_0 = 3.6899$**

Fig. 6. shows commutative detected cases of malaria as reported in Zimbabwe. We used the 52 weekly reports of malaria cases to fit in the model system (2.1). From the results we can note for

the first 30 weeks estimates from fractional-order model deviates from the reported cases of real data and thereafter estimates significantly better forecasts of the disease for the 35 to 52 weeks. Overall we conclude that in a long range interaction of vectors and hosts fractional order model present better forecasts of dynamics of malaria disease in the population.

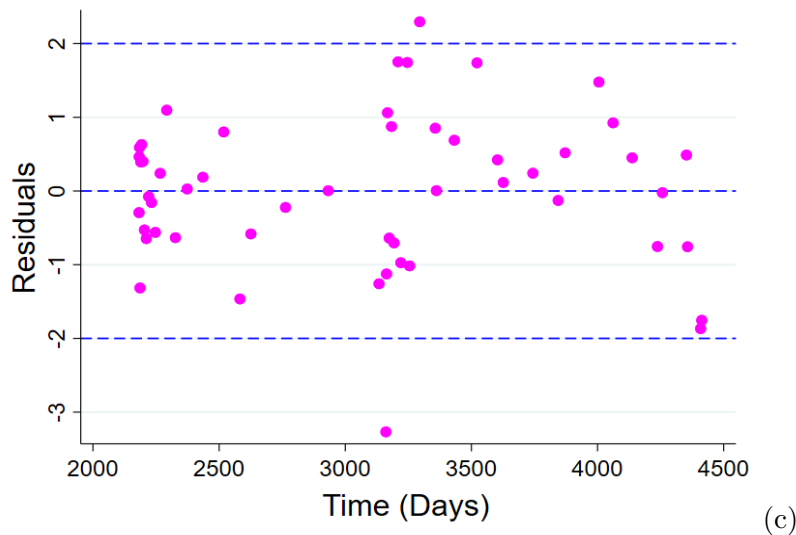


Fig. 7. Graphical representation of residuals against time for malaria cases in Zimbabwe for the model system (2.1)

Fig. 7. shows the graphical representation of residuals of the model system (2.1) for 52 weekly reports of malaria cases reported in Zimbabwe. Overall we can conclude that the residuals did not follow any particular path (exhibited random pattern) which shows that the fractional-order model (2.1) present better forecasts to the reported real data of malaria cases in Zimbabwe. This result is more reliable and realistic which is inline to that in [48] published.

### 3.4 Simulation of the model to support the analytical results

In this section, we simulated the model (2.1) at  $\alpha \in (0, 1]$  to support the analytical results. We first simulate the model at  $\mathcal{R}_0 < 1$ , followed by simulation at  $\mathcal{R}_0 > 1$  to show the behavior of dynamical solution in a long-range of interaction between humans and mosquitoes. Numerical simulation in Fig. 8. shows the convergence of model solutions to the disease-free equilibrium with different derivative orders. The solution were obtained upon setting  $\theta_h = 0.4$ ,  $\sigma_h = 0.05$ ,  $\epsilon_h = 0.4$ ,  $\Lambda_{h1} = \Lambda_{h2} = 0.00001$ ,  $\rho = 0.005$ ,  $\Lambda_v = 0.001$ . giving  $\mathcal{R}_0 = 0.0013$ . Overall, we can note that as the order of derivative approaches unit the time taken by the solution to converge to the disease-free equilibrium increases.

Numerical simulation in Fig. 9 shows the dynamical solutions of infected humans and mosquitoes for  $\mathcal{R}_0 = 3.6899$ . Overall we can observe that in a long range interaction of humans and mosquitoes, the solution profiles are associated with periodic oscillations. The implication of results is that inclusion of asymptotic individuals in the population destabilize the solution of model system leads to periodic outbreaks of malaria disease in the population. Additionally, we can note that whenever the derivative order  $\alpha$  is reduced from 1, the memory effect of the system increases, as a result the number of infected mosquitoes and humans increase over time.

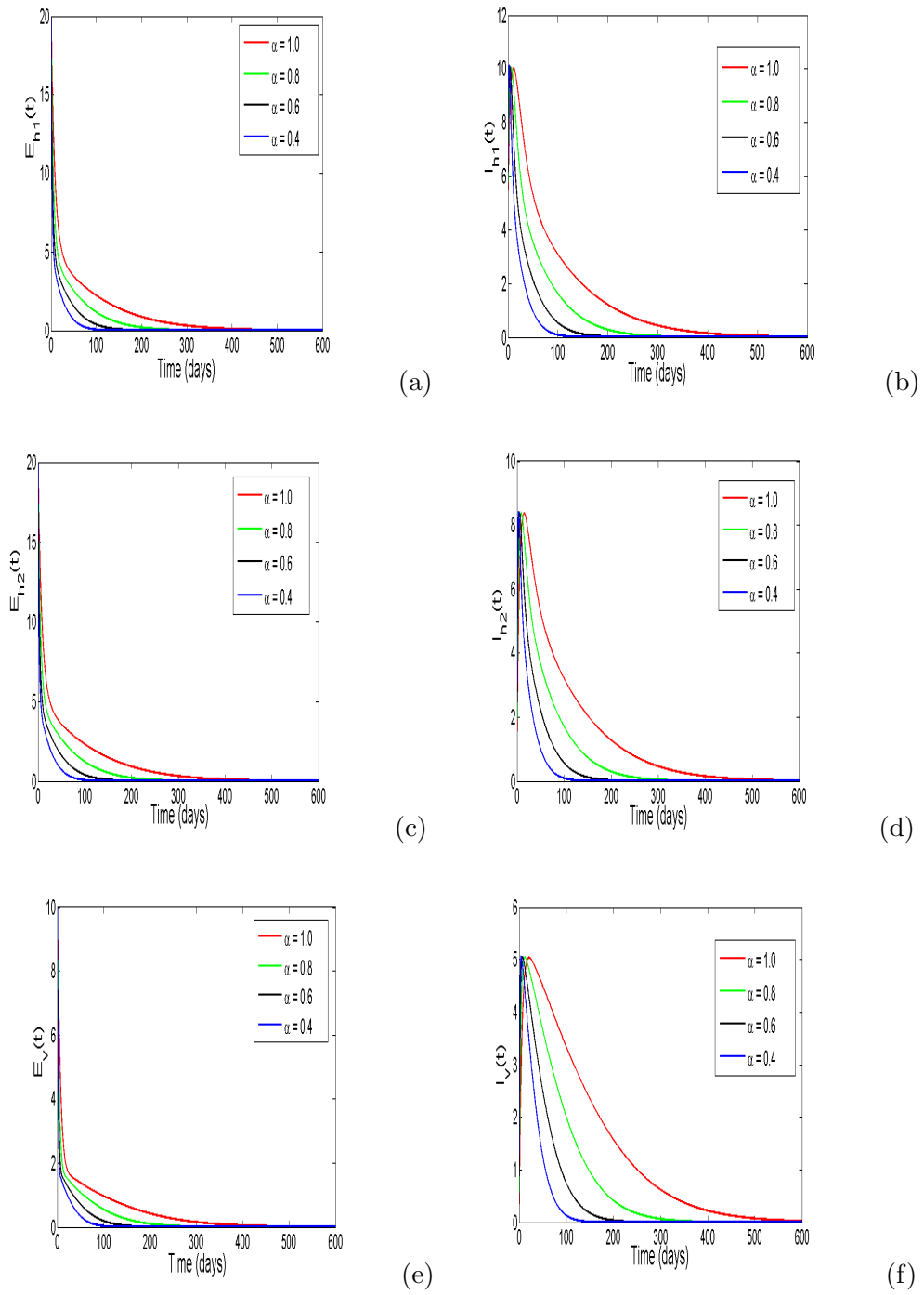
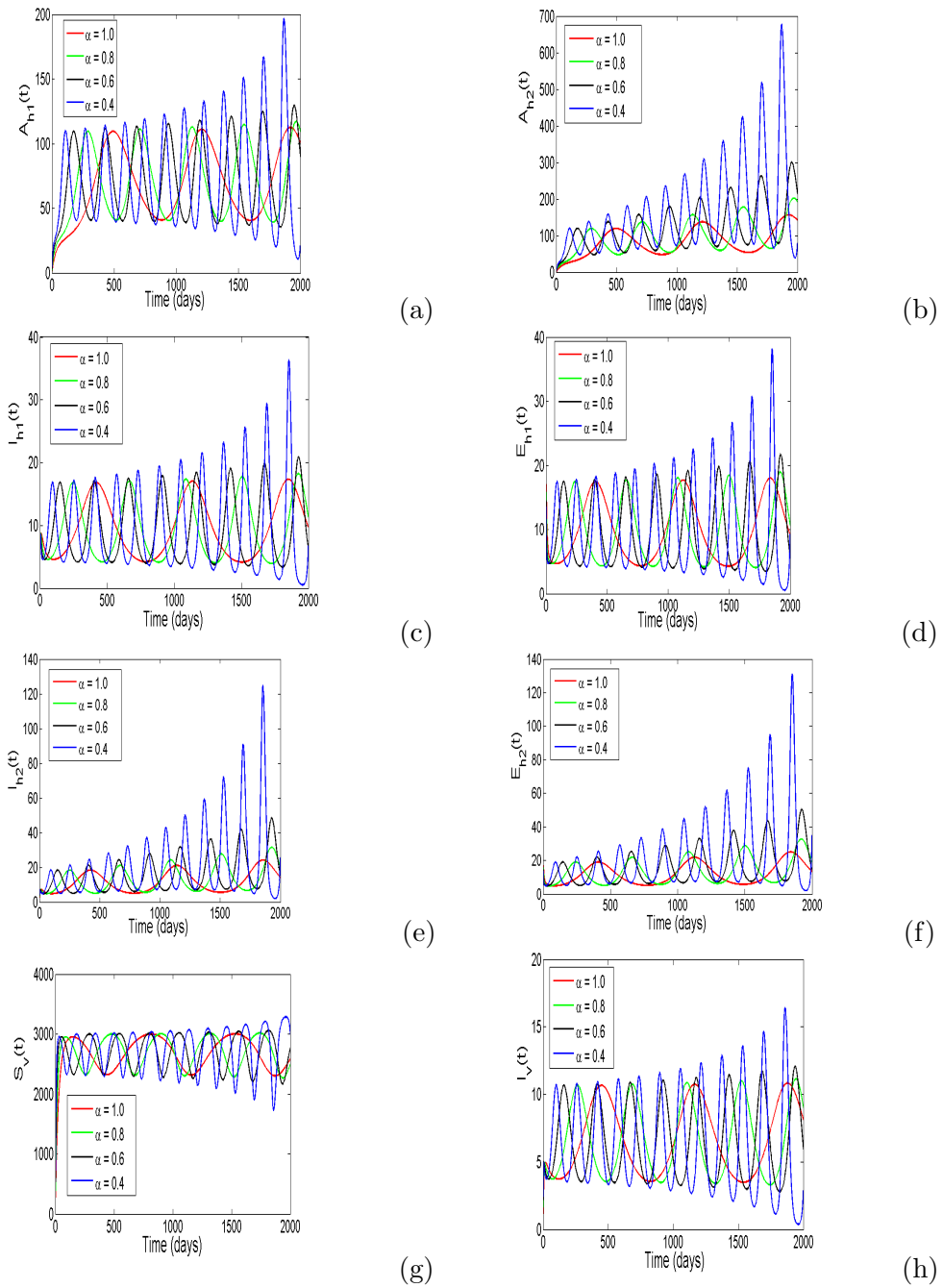


Fig. 8. Dynamical solutions of model system (2.1) with different order derivatives



**Fig. 9. Dynamical solutions of model system (2.1) with different order derivatives.**  
**The solutions were obtained upon setting**  
 $\theta_h = 0.4$ ,  $\sigma_h = 0.05$ ,  $\epsilon_h = 0.4$ ,  $\Lambda_{h1} = \Lambda_{h2} = 0.00001$ ,  $\rho = 0.005$ , and  $\Lambda_v = 0.001$  giving  $\mathcal{R}_0 = 3.6899$ .



## 4 Conclusions

In this study we proposed and analyzed a new fractional-order derivative model of malaria disease transmission using Atangana-Baleanu in Caputo sense. In the model analysis we computed the basic reproduction number  $\mathcal{R}_0$  and showed that whenever  $\mathcal{R}_0 < 1$  the disease dies out in the population and persists whenever  $\mathcal{R}_0 > 1$ . We proved the existence and give the criteria for uniqueness of the model solution using Lipschitz condition and Banach fixed point theorem. In numerical simulations, We used the nonlinear least square method to perform the parameters estimation and fit the model with real data of malaria disease reported in Zimbabwe. The results showed that the model fits well with reported malaria cases and more relevant to those published inline[56]. We performed the sensitivity analysis of the model parameters to determine the correlation between the model parameters and  $\mathcal{R}_0$ . Overall, we noted that parameters  $\Lambda_v, \beta_h, \beta_v, \sigma, \gamma_u, \gamma_v$  and  $\alpha_h$  have a strongly correlation to the threshold quantity  $\mathcal{R}_0$ . Finally, we used the Adam-Bashforth-Moulton scheme to simulate the model. Overall, we noted that whenever the derivative order  $\alpha$  is approaches 1, the memory effects of infected vectors and humans increase as a results that the number of oscillations increases overtime. The findings in this study is more useful in health authorities specifically in developing countries where malaria disease is still endemic in most areas. In future, this model can be extended and include the human and vector migrations and assess their effects on spread of malaria disease in the population.

## Acknowledgment

We would like to thank the anonymous referees and the editors for their invaluable time used to handle the manuscript.

## Competing Interests

Authors have declared that no competing interests exist.

## References

- [1] Talapko J, Škrlec I, Alebić T, Jukić M, Včev A. Malaria: the past and the present. *Microorganisms*. 2019;7 (6): 179.
- [2] Oke SI, Ojo MM, Adeniyi MO, Matadi MB. Mathematical modeling of malaria disease with control strategy. *Commun. Math. Biol. Neurosci*. 2020;2020:Article-ID.
- [3] Okosun KO, Makinde OD. A co-infection model of malaria and cholera diseases with optimal control. *Mathematical biosciences*. 2014;258:19-32.
- [4] Forouzannia F, Gumel AB. Mathematical analysis of an age-structured model for malaria transmission dynamics. *Mathematical biosciences*. 2014;247:80-94.
- [5] Gimba B, Bala SI. Modeling the impact of bed-net use and treatment on malaria transmission dynamics. *International Scholarly Research Notices*. 2017;2017.
- [6] Helikumi, Mlyashimbi and Kgosimore, Moatlhodi and Kuznetsov, Dmitry and Mushayabasa, Steady. Dynamical and optimal control analysis of a seasonal *Trypanosoma brucei rhodesiense* model. *Mathematical Biosciences and Engineering*. 2020 ;17(3):2530-2556.
- [7] Liao X, Lin D, Dong L, Ran M, Yu D. Analog Implementation Of Fractional-Order Electric Elements Using Caputo’s Fabrizio And Atangana’s Baleanu Definitions. *FRACTALS (fractals)*. 2021;29(07):1-4.
- [8] Coelho CH, Doritchamou JY, Zaidi I, Duffy PE. Advances in malaria vaccine development: report from the 2017 malaria vaccine symposium; 2017.

- [9] Okyere E, Oduro FT, Amponsah SK, Dontwi IK. Fractional order optimal control model for malaria infection. arXiv preprint arXiv:1607.01612; 2016 .
- [10] Sweilam NH, AL-Mekhlafi SM, Albalawi AO. Optimal control for a fractional order malaria transmission dynamics mathematical model. Alexandria Engineering Journal. 2020;59(3):1677-92.
- [11] Agarwal M, Bhadauria AS. A stage structured model of malaria transmission and efficacy of mosquito larvicides in its control. International Journal of Modeling, Simulation, and Scientific Computing. 2014;5(04):1450023.
- [12] Atangana A, Qureshi S. Mathematical modeling of an autonomous nonlinear dynamical system for malaria transmission using Caputo derivative. Fractional order analysis: Theory, methods and applications. 2020;225-52.
- [13] Bichara D, Castillo-Chavez C. Vector-borne diseases models with residence times—a lagrangian perspective. Mathematical biosciences. 2016;281:128-38.
- [14] Singh R, Abdeljawad T, Okyere E, Guran L. Modeling, analysis and numerical solution to malaria fractional model with temporary immunity and relapse. Advances in Difference Equations. 2021;2021(1):1-27.
- [15] Boukhouima A, Hattaf K, Lotfi EM, Mahrouf M, Torres DF, Yousfi N. Lyapunov functions for fractional-order systems in biology: Methods and applications. Chaos, Solitons Fractals. 2020;140:110224.
- [16] Ghosh M, Lashari AA, Li XZ. Biological control of malaria: A mathematical model. Applied Mathematics and Computation. 2013;219(15):7923-39.
- [17] Kumar D, Singh J, Al Qurashi M, Baleanu D. A new fractional SIRS-SI malaria disease model with application of vaccines, antimalarial drugs, and spraying. Advances in Difference Equations. 2019;2019(1):1-9.
- [18] Lashari AA, Hattaf K, Zaman G, Li XZ. Backward bifurcation and optimal control of a vector borne disease. Applied Mathematics Information Sciences. 2013;7(1):301-9.
- [19] Olaniyi S, Mukamuri M, Okosun KO, Adepoju OA. Mathematical analysis of a social hierarchy-structured model for malaria transmission dynamics. Results in Physics. 2022;34:104991.
- [20] Prosper O, Ruktanonchai N, Martcheva M. Optimal vaccination and bednet maintenance for the control of malaria in a region with naturally acquired immunity. Journal of theoretical biology. 2014;353:142-56.
- [21] Otieno G, Koske JK, Mutiso JM. Transmission dynamics and optimal control of malaria in Kenya. Discrete Dynamics in Nature and Society. 2016;2016.
- [22] Yavuz M, Bonyah E. New approaches to the fractional dynamics of schistosomiasis disease model. Physica A: Statistical Mechanics and its Applications. 2019;525:373-93.
- [23] Alkahtani BS. Atangana-Batogna numerical scheme applied on a linear and non-linear fractional differential equation. The European Physical Journal Plus. 2018;133(3):1-10.
- [24] Atangana A, Owolabi KM. New numerical approach for fractional differential equations. Mathematical Modelling of Natural Phenomena. 2018;13(1):3.

- [25] Abboubakar H, Kumar P, Rangaig NA, Kumar S. A malaria model with Caputo–Fabrizio and Atangana–Baleanu derivatives. *International Journal of Modeling, Simulation, and Scientific Computing*. 2021;12(02):2150013.
- [26] Toufik M, Atangana A. New numerical approximation of fractional derivative with non-local and non-singular kernel: application to chaotic models. *The European Physical Journal Plus*. 2017;132(10):1-6.
- [27] Akyildiz FT, Alshammari FS. Complex mathematical SIR model for spreading of COVID-19 virus with Mittag-Leffler kernel. *Advances in difference equations*. 2021;2021(1):1-17.
- [28] Khan MA, Ullah S, Farooq M. A new fractional model for tuberculosis with relapse via Atangana–Baleanu derivative. *Chaos, Solitons Fractals*. 2018;116:227-38.
- [29] Ali A, Islam S, Khan MR, Rasheed S, Allehiany FM, Baili J, Khan MA, Ahmad H. Dynamics of a fractional order Zika virus model with mutant. *Alexandria Engineering Journal*. 2022;61(6):4821-36.
- [30] Simelane SM, Dlamini PG. A fractional order differential equation model for hepatitis B virus with saturated incidence. *Results in Physics*. 2021;24:104114.
- [31] Abu Arqub O, Singh J, Alhodaly M. Adaptation of kernel functions-based approach with Atangana–Baleanu–Caputo distributed order derivative for solutions of fuzzy fractional Volterra and Fredholm integrodifferential equations. *Mathematical Methods in the Applied Sciences*; 2021.
- [32] Shikrani R, Hashmi MS, Khan N, Ghaffar A, Nisar KS, Singh J, Kumar D. An efficient numerical approach for space fractional partial differential equations. *Alexandria Engineering Journal*. 2020;59(5):2911-9.
- [33] Owolabi KM, Atangana A. On the formulation of Adams-Bashforth scheme with Atangana–Baleanu–Caputo fractional derivative to model chaotic problems. *Chaos: An Interdisciplinary Journal of Nonlinear Science*. 2019;29(2):023111.
- [34] Naik PA, Owolabi KM, Zu J, Naik MU. Modeling the transmission dynamics of COVID-19 pandemic in Caputo type fractional derivative. *Journal of Multiscale Modelling*. 2021;12(03):2150006.
- [35] Helikumi M, Eustace G, Mushayabasa S. Dynamics of a Fractional-Order Chikungunya Model with Asymptomatic Infectious Class. *Computational and Mathematical Methods in Medicine*. 2022;2022.
- [36] Shah SA, Khan MA, Farooq M, Ullah S, Alzahrani EO. A fractional order model for Hepatitis B virus with treatment via Atangana–Baleanu derivative. *Physica A: Statistical Mechanics and its Applications*. 2020;538:122636.
- [37] Guo Y, Li T. Modeling and dynamic analysis of novel coronavirus pneumonia (COVID-19) in China. *Journal of Applied Mathematics and Computing*. 2021:1-26.
- [38] Bonyah EB. Fractional optimal control for a corruption model. *J. Prime Res. Math*. 2020;16(1):11-29.
- [39] Almalahi MA, Ibrahim AB, Almutairi A, Bazighifan O, Aljaaidi TA, Awrejcewicz J. A qualitative study on second-order nonlinear fractional differential evolution equations with generalized ABC operator. *Symmetry*. 2022;14(2):207.
- [40] Almalahi MA, Panchal SK, Shatanawi W, Abdo MS, Shah K, Abodayeh K. Analytical study of transmission dynamics of 2019-nCoV pandemic via fractal fractional operator. *Results in Physics*. 2021;24:104045.
- [41] Butt AI, Ahmad W, Rafiq M, Baleanu D. Numerical analysis of Atangana–Baleanu fractional model to understand the propagation of a novel corona virus pandemic. *Alexandria Engineering Journal*. 2022;61(9):7007-27.

- [42] Cai L, Li X, Tuncer N, Martcheva M, Lashari AA. Optimal control of a malaria model with asymptomatic class and superinfection. *Mathematical biosciences*. 2017;288:94-108.
- [43] Ahmed I, Modu GU, Yusuf A, Kumam P, Yusuf I. A mathematical model of Coronavirus Disease (COVID-19) containing asymptomatic and symptomatic classes. *Results in physics*. 2021;21:103776.
- [44] Sinan M, Ahmad H, Ahmad Z, Baili J, Murtaza S, Aiyashi MA, Botmart T. Fractional mathematical modeling of malaria disease with treatment insecticides. *Results in Physics*. 2022;34:105220.
- [45] Sardar T, Saha B. Mathematical analysis of a power-law form time dependent vector-borne disease transmission model. *Mathematical biosciences*. 2017;288:109-23.
- [46] Cai L, Li X, Tuncer N, Martcheva M, Lashari AA. Optimal control of a malaria model with asymptomatic class and superinfection. *Mathematical biosciences*. 2017;288:94-108.
- [47] Ndong AM, Munganga JM, Mwambakana JN, Saad-Roy CM, Van den Driessche P, Walo RO. Analysis of a model of gambiense sleeping sickness in humans and cattle. *Journal of biological dynamics*. 2016;10(1):347-65.
- [48] Helikumi M, Eustace G, Mushayabasa S. Dynamics of a Fractional-Order Chikungunya Model with Asymptomatic Infectious Class. *Computational and Mathematical Methods in Medicine*. 2022;2022.
- [49] Abboubakar, Hamadjam and Kumar, Pushpendra, Rangaig, Norodin A, Kumar, Sachin, "International Journal of Modeling, Simulation, and Scientific Computing. *International Journal of Modeling, Simulation, and Scientific Computing*. 2021;12(02):2150013.
- [50] Helikumi M, Kgosimore M, Kuznetsov D, Mushayabasa S. A fractional-order Trypanosoma brucei rhodesiense model with vector saturation and temperature dependent parameters. *Advances in Difference Equations*. 2020;2020(1):1-23.
- [51] Diethelm Kai. The analysis of fractional differential equations: An application-oriented exposition using differential operators of Caputo type. Springer Science and Business Media; 2020.
- [52] Toufik M, Atangana A. New numerical approximation of fractional derivative with non-local and non-singular kernel: application to chaotic models. *The European Physical Journal Plus*. 2017;132(10):1-6.
- [53] Pinto CM, Machado JT. Fractional model for malaria transmission under control strategies. *Computers Mathematics with Applications*. 2013;66(5):908-16.
- [54] Singh J, Kumar D, Baleanu D. New aspects of fractional Bloch model associated with composite fractional derivative. *Mathematical Modelling of Natural Phenomena*. 2021;16:10.
- [55] Purwati, Utami Dyah, Nainggolan, Jonner et al., Parameter estimation and sensitivity analysis of malaria model. *Journal of Physics: Conference Series*. 2020;1490(1):012039.
- [56] Mukhtar, Abdulaziz Yagoub Abdelrahman. Mathematical modeling of the transmission dynamics of malaria in South Sudan. University of the Western Cape; 2019.
- [57] Shaw, W Robert and Holmdahl, Inga E and Itoe, Maurice A and Werling, Kristine and Marquette, Meghan and Paton, Douglas G and Singh, Naresh and Buckee, Caroline O and Childs, Lauren M and Catteruccia, Flaminia. Current estimates of malaria basic reproduction number underestimate parasite transmission efficiency due to multiple blood feeding. Cold Spring Harbor Laboratory. 2020;2020-03.
- [58] Abboubakar, Hamadjam and Kumar, Pushpendra, Rangaig, Norodin A, Kumar, Sachin, "International Journal of Modeling, Simulation, and Scientific Computing. *International Journal of Modeling, Simulation, and Scientific Computing*. 2021;12(02):2150013.

- [59] Pan F, Cui X, Xue D, Lu Z. Stability analysis of a fractional-order vector-bias model on malaria transmission. In 2019 Chinese Control And Decision Conference (CCDC). 2019;6363-6367. IEEE.

---

© 2022 Helikumi and Lolika; This is an Open Access article distributed under the terms of the Creative Commons Attribution License (<http://creativecommons.org/licenses/by/4.0>), which permits unrestricted use, distribution, and reproduction in any medium, provided the original work is properly cited.

**Peer-review history:**

The peer review history for this paper can be accessed here (Please copy paste the total link in your browser address bar)

<https://www.sdiarticle5.com/review-history/88271>